Dalton
Transactions

An international journal of inorganic chemistry

rsc.li/dalton

Volume 46
Number 10
14 March 2017
Pages 3073-3412

COMMUNICATION
Douglas W. Stephen et al
N-Heterocyclic carbene stabilized parent sulfenyl, selenenyl, and tellurenyl cations (XH⁺; X = S, Se, Te)

ISSN 0306-0012

ROYAL SOCIETY OF CHEMISTRY

ROYAL SOCIETY OF CHEMISTRY

rsc.li/dalton

Catalytic intramolecular hydroamination of aminoallenes using titanium and tantalum complexes of sterically encumbered chiral sulfonamides

Fanrui Sha[†], Emily A. Shimizu[†], Hannah S. Slocumb[†], Sydney E. Towell[†], Yi Zhen[†], Hanna Z. Porter[†], Michael K. Takase[‡], and Adam R. Johnson[†,*]

[†]Harvey Mudd College, 301 Platt Blvd., Claremont, CA 91711

[‡]Beckman Institute, California Institute of Technology, Pasadena, CA 91125

Abstract

Catalysis using earth abundant metals is an important goal due to the relative scarcity and expense of precious metal catalysts. It would be even more beneficial to use earth abundant catalysts for the synthesis of common pharmaceutical structural motifs such as pyrrolidine and pyridine. Thus, developing titanium catalysts for asymmetric ring closing hydroamination is a valuable goal. In this work, four sterically encumbered chiral sulfonamides derived from naturally occurring amino acids were prepared. These compounds undergo protonolysis reactions with $Ti(NMe_2)_4$ or $Ta(NMe_2)_5$ to give monomeric complexes as determined by both DOSY NMR and X-ray crystallography. The resulting complexes are active for the ring closing hydroamination hepta-4,5-dienylamine to give a mixture of tetrahydropyridine and pyrrolidine products. However, the titanium complexes convert 6-methylhepta-4,5-dienylamine exclusively to 2-(2-methylpropenyl)pyrrolidine in higher enantioselectivity than those previously reported, with enantiomeric excesses ranging from 18-

24%. The corresponding tantalum complexes were more selective with enantiomeric excesses ranging from 33-39%.

Introduction

Hydroamination, the direct addition of an N-H bond across an unsaturated carbon-carbon bond, is an atom-economical transformation that can result in both piperidine and pyrrolidine heterocycles that are commonly found in US FDA approved pharmaceuticals.[1] Metals from across the periodic table have been investigated as catalysts for this transformation,[2-8] including late metals[9-11] and lanthanides.[12-13] The development of earth-abundant catalysts has lately become an important goal.[14-16] Many groups are developing catalysts based on group-IV and -V metals for both hydroamination and the related hydroaminoalkylation reactions.[17-42] The reaction has been under intense study, but general procedures for hydroamination remain to be realized.

Gold catalysts have been shown to be capable of highly enantioselective hydroamination of aminoallenes to give pyrrolidines, but the substrates must be *N*-tosylated.[43] Ideally, this reaction would be achieved using less expensive catalysts and without the necessity of protecting groups. Thus, our goal has been to develop a low-cost, earth-abundant catalyst for the transformation of the unprotected substrates. Our group has studied the intramolecular hydroamination of both di- and trisubstituted aminoallene substrates (Scheme 1, compounds **1a** and **1b**) using the early transition metals titanium and tantalum.[44-46] We have found that substrate **1a** can give a mixture of tetrahydropyridine **2a** and pyrrolidine **3a** products, while substrate **1b** gives only the pyrrolidine product **3b**.
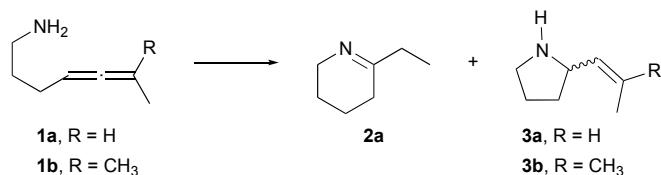
Scheme 1 Catalytic hydroamination of di- and trisubstituted aminoallenes (**1**) gives achiral tetrahydropyridine (**2a**) or chiral α-vinylpyrrolidines (**3a** and **3b**).

We have observed that tantalum catalysts perform better than their corresponding titanium catalysts in this hydroamination reaction. Tantalum derived catalysts have achieved enantioselectivities up to 80% ee,[45] although the highest enantioselectivity we have observed for a titanium derived catalyst is below 20% ee.[46-47] We have obtained several crystal structures of titanium complexes with bidentate amide-alkoxide ligands, and all of them are dimeric with bridging oxygen atoms.[48-49] The crystal structures of tantalum complexes we have obtained have all been monomeric.[45, 50] Interestingly, the highest enantioselectivity we have observed with a titanium catalyst was with a ligand that contained an additional donor atom resulting in a monomeric species.[46] This result led us to postulate that if the dimeric nature of the titanium complexes was maintained in solution, a possible explanation for the reduced selectivity for the titanium complexes relative to their tantalum counterparts is their dimeric nature.

Our group has focused on using "chiral-pool"[51] derived ligands based principally on the naturally occurring amino acids phenylalanine and valine. We published a series of sulfonamide ligands in 2011.[52] The ligands in that publication had only H and Me substituents α to the oxygen, while ligands containing Ph substituents at that position have generally been more selective.[47] Sulfonamides are known to sometimes coordinate to titanium centers through a sulfonamide oxygen,[53-60] and this additional coordination site could lead to different reactivity,

especially with the larger phenyl substituent that can project the ligand chirality more efficiently. With a sterically more encumbered sulfonamide ligand, we hoped to observe two results: first, the isolation of monomeric titanium complexes, and second, increased stereoselectivity for the hydroamination of aminoallene substrates.

Results and Discussion

Synthesis of ligands

The synthesis of the ligands followed procedures similar to those reported previously.[52, 54-58] Treatment of the phenylalanine-derived amino alcohol (*S*)-2-amino-1,1,3-triphenylpropanol with a substituted aryl sulfonyl chloride gave the desired sulfonamides in good yield. Spectroscopic data for sulfonamide L-H$_2$**Ph1** matched the literature.[61] All compounds were purified either by recrystallization (H$_2$**Ph1** and H$_2$**Ph2**) or by chromatography (H$_2$**Ph3** and H$_2$**Ph4**). The D-enantiomers of H$_2$**Ph2** and H$_2$**Ph3** were also prepared to verify enantiopurity of the sulfonamides. Chiral contact shift NMR spectroscopy showed no evidence of racemization during their synthesis. Plots of the contact shift NMR studies are presented in the ESI.
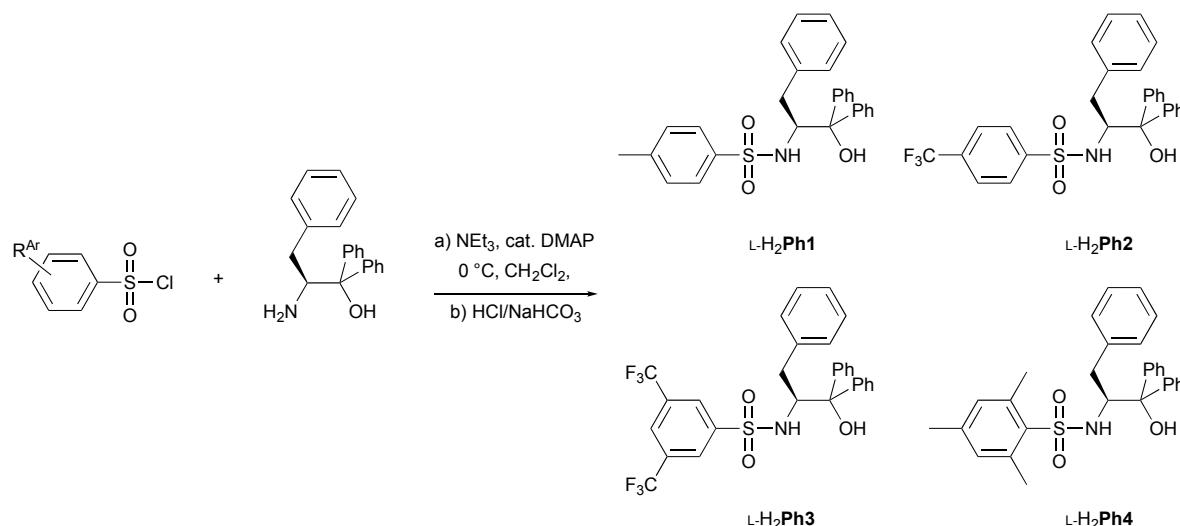
Scheme 2 Synthesis of sulfonamides used in this study.

Attempts were made to prepare the even bulkier 2,4,6-tri-isopropyl sulfonamide. Two

products, both with similar NMR chemical shifts were observed. Although the two products

could be separated by column chromatography, the yield of the desired sulfonamide was low.

IR spectroscopy suggested that the major product was the corresponding sulfonate ester as it

contained S-O stretches but no S-N stretch near 950 cm^{-1}.[62] Additional attempts at increasing

bulk at the 2,6-positions of the aromatic ring were thus abandoned. IR stretches consistent with

the sulfonamide group were observed in all four compounds.[63]

XRD of Ph1

A single crystal of L-H$_2$**Ph1** was grown by slow evaporation from ethanol. The molecular

structure is shown in Figure 1, and crystallographic parameters are listed in the ESI (Table S1).

The molecule crystallizes with two molecules in the asymmetric unit that are essentially

isostructural; both molecules are shown in the ESI (Figure S1). The crystal structures of amino

alcohol ligands we have obtained previously often contain intramolecular hydrogen bonds,[64]

even with diphenyl substitution on the tertiary alcohol carbon.[65] However, this molecule has no

intramolecular hydrogen bonds but has several intermolecular ones. There are two short

contacts linking N(1)H(1A)···O(5), a sulfonyl oxygen, at 2.088 Å and O(4)H(4)···O(3) at 2.021 Å.

There are two longer contacts, N(2)H(2A)···O(1) at 2.280 Å and O(1)H(1)···O(4) at 2.281 Å. These

contacts form a zig-zag structure in the ab plane. There are no other short contacts observed. A

view of the hydrogen bonding network is shown in the ESI (Figure S2).
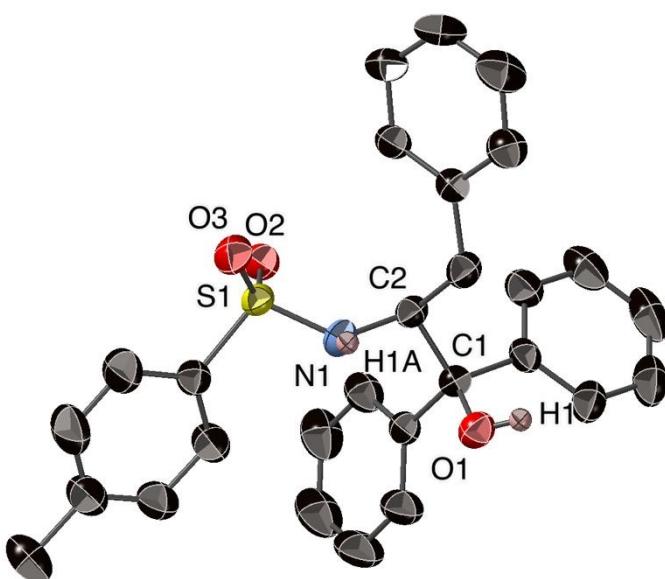
Figure 1. Thermal ellipsoid drawing of **ʟ-H₂Ph1** (all hydrogen atoms except H(1A) and H(1) omitted for clarity; ellipsoids shown at 50% probability).

Synthesis of complexes

Titanium complexes of the ʟ-enantiomers of **Ph1**, **Ph2**, and **Ph3** were prepared by adding

a chilled ether solution of the ligand to a chilled ether solution of Ti(NMe₂)₄ (Scheme 3). The

titanium complexes appeared red in solution but were isolated as yellow solids that

precipitated from the reaction solution in moderate yields due to their high solubility in ether.

The complexes could be isolated essentially quantitatively in impure form by removing the

solvent and subsequently purified by recrystallization from toluene. All three complexes were

isolated as the dimethylamine adducts.
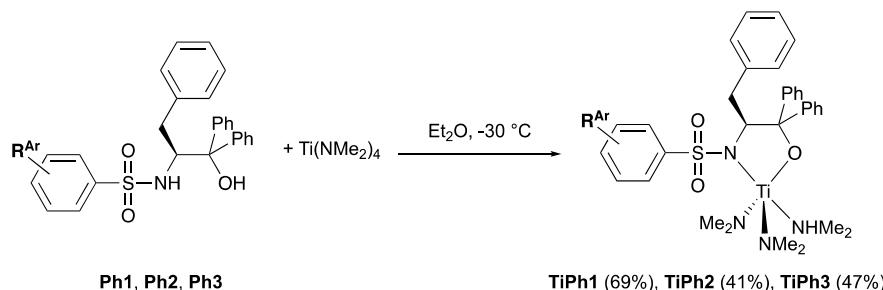
Scheme 3 Synthesis of titanium sulfonamide complexes; **TiPh1**, R^{Ar} = 4-CH$_3$, **TiPh2**, R^{Ar} = 4-CF$_3$, **TiPh3**, R^{Ar} = 3,5-di-CF$_3$.

Since H$_2$**Ph1** is relatively insoluble in ether, the synthesis of complex **TiPh1** was also attempted in dichloromethane, but this resulted in several unknown side products. Complex **TiPh2** shows coordinated dimethylamine in both the ^{1}H and ^{13}C NMR spectra, but the elemental analysis results are consistent with loss of the coordinated amine. Attempts to heat solutions of **TiPh2** and evacuate the headspace to drive off the amine were not successful as determined by ^{1}H NMR spectroscopy. Complex **TiPh3** tenaciously retains toluene after recrystallization, and the ^{1}H, ^{13}C NMR spectra, elemental analysis results, and X-ray crystal structure (*vide infra*) are all consistent with a toluene of solvation. Attempts to remove the toluene under vacuum were unsuccessful.

The titanium complex of **Ph4** could not be prepared by simply stirring overnight in ether. A series of NMR tube scale reactions showed that it took approximately three days at 65 °C for complete conversion to the desired product. It is possible that the steric bulk of the 2,6-dimethyl substituents prevents ready complexation. For preparative scale synthesis, the reaction was carried out in toluene in a Teflon sealed glass reaction vessel. Complex **TiPh4** was isolated as an orange-brown foam in 95% yield and was characterized by ^{1}H and ^{13}C NMR

spectroscopy, but attempts to crystallize the material have thus far been unsuccessful (Scheme

4). Complex **TiPh4** did not retain dimethylamine.
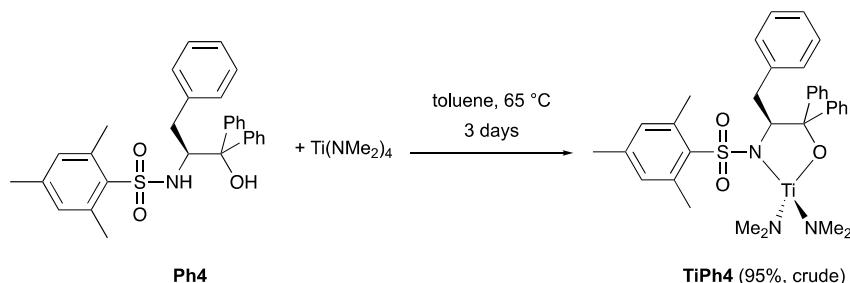
Scheme 4 Synthesis of **TiPh4**.

All four titanium complexes exhibit two inequivalent NMe_2 resonances at around 2.8

and 3.2 ppm, and **TiPh1**, **TiPh2**, and **TiPh3** also have an additional resonance for the

coordinated $HNMe_2$ ligand as a doublet at around 1.8 ppm in their ^1H NMR spectra. **TiPh2** and

TiPh3 exhibit sharp singlets in their ^{19}F NMR spectra for the CF_3 groups. The spectroscopic data

are consistent with the formulation of the complexes as Ti(**Ph1-3**)$(NMe_2)_2(HNMe_2)$ and

Ti(**Ph4**)$(NMe_2)_2$.

The synthesis of the tantalum complexes was straightforward and followed a similar

procedure to that of their titanium analogs. Addition of a chilled ether solution of the ligand to

a chilled ether solution of Ta$(NMe_2)_5$ resulted in essentially quantitative yield of the desired

complexes as white to off-white solids after an overnight reaction (Scheme 5). All four

complexes could be purified by recrystallization from ether in low yields.

TaPh1 (100%), **TaPh2** (100%),
TaPh3 (99%), **TaPh4** (100%)
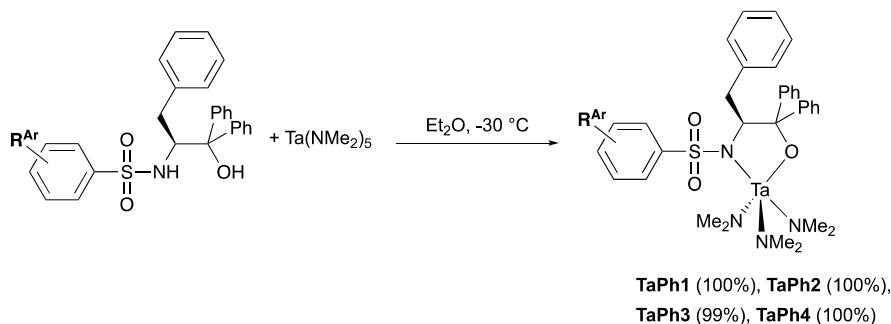
Scheme 5 Synthesis of tantalum sulfonamide complexes; **TaPh1**, R^{Ar} = 4-CH$_3$, **TaPh2**, R^{Ar} = 4-CF$_3$, **TaPh3**, R^{Ar} = 3,5-di-CF$_3$, **TaPh4**, R^{Ar} = 2,4,6-tri-CH$_3$.

The tantalum complexes all exhibit sharp singlets for the NMe$_2$ groups at around 3.2 ppm in their ^{1}H NMR spectra. **TaPh2** and **TaPh3** exhibit sharp singlets in their ^{19}F NMR spectra. All spectroscopic data are consistent with their formulation as Ta(Ph1-4)(NMe$_2$)$_3$. The elemental analysis results for **TaPh3** suggest that two dimethylamide ligands were replaced by an oxo group. The elemental analysis results for **TaPh4** are consistent with one dimethylamide ligand being replace by a hydroxide. These results are presumably due to sample handling as the NMR spectra are consistent with the expected formulation.

X-Ray structures of complexes

X-ray quality crystals of **TiPh3**, **TaPh1**, **TaPh2** and **TaPh3** were obtained from a chilled ether solution of the complex. Suitable crystals were mounted at 100 K and their structures were determined. Crystallographic parameters are listed in the ESI (Table S1). The geometry around the titanium center is best described as a distorted trigonal bipyramid with R$_c$(x) parameter of 9.77 for trigonal bipyramidal and 21.44 for square pyramidal.[66] The τ parameter is 0.53,[67] or 53% of the way from perfectly tetragonal to perfectly trigonal. The TBP axis is between the ligand nitrogen N(1) and the NHMe$_2$ nitrogen N(2). There is one short contact (3.085 Å) from the hydrogen atom on the dimethylamine to O(2) on adjacent molecule. **TiPh3**

crystallizes with one molecule of toluene in the asymmetric unit, consistent with the

spectroscopic and analysis data. The CF_3 groups were modeled as two component disorders. A

complete ORTEP with disordered CF_3 groups and the toluene of crystallization is shown in the

ESI (Figure S3).
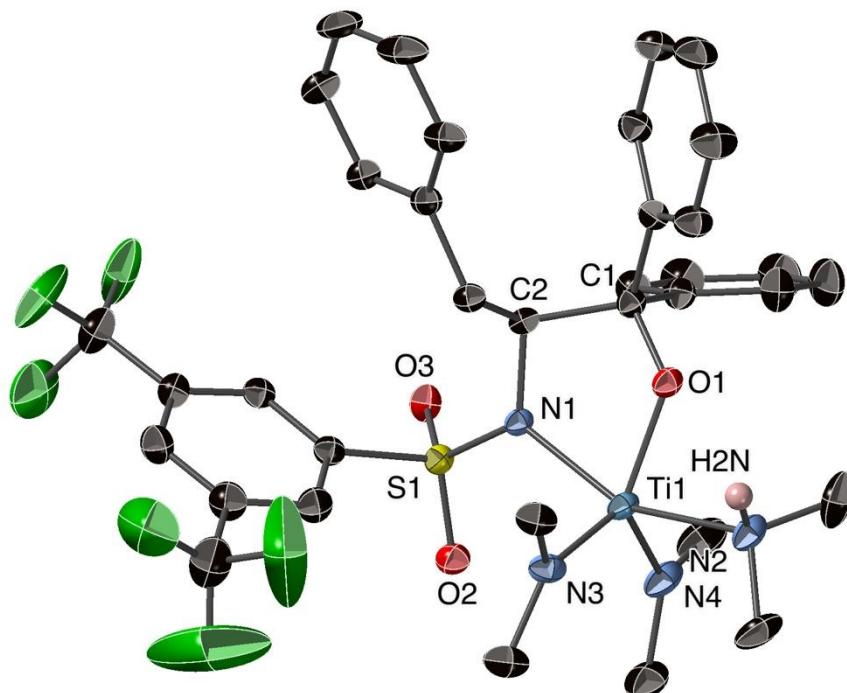
Figure 2. Thermal ellipsoid drawing of complex **TiPh3** (toluene molecule and all hydrogen atoms except H(2N) are omitted for clarity; ellipsoids shown at 50% probability). Selected bond distances (Å) and angles (°): Ti(1)-N(4) 1.877(2), Ti(1)-O(1) 1.8866(18), Ti(1)-N(3) 1.908(2), Ti(1)-N(1) 2.115(2), Ti(1)-N(2) 2.224(2), N(4)-Ti(1)-O(1) 120.39(10), N(4)-Ti(1)-N(3) 115.90(11), O(1)-Ti(1)-N(3) 123.36(9), N(4)-Ti(1)-N(1) 101.47(9), O(1)-Ti(1)-N(1) 75.91(8), N(3)-Ti(1)-N(1) 99.22(9), N(4)-Ti(1)-N(2) 94.95(10), O(1)-Ti(1)-N(2) 79.82(8), N(3)-Ti(1)-N(2) 89.95(10), N(1)-Ti(1)-N(2) 155.24(9).

All three tantalum complexes are essentially isostructural with only minor variations in

bond angles around the tantalum and orientation of the dimethylamide groups. The structures

of **TaPh1** and **TaPh2** are reported in the ESI (Figures S4 and S5). Like **TiPh3**, the geometry

around the tantalum center in **TaPh3** is also best described as a distorted trigonal bipyramid. It

has an $R_c(x)$ parameter of 11.04 for trigonal bipyramidal and 17.88 for square pyramidal,[66] with

a τ parameter of 0.35.[67] The TBP axis is between the ligand nitrogen N(1) and the NMe_2

nitrogen N(2) (Figure 3).
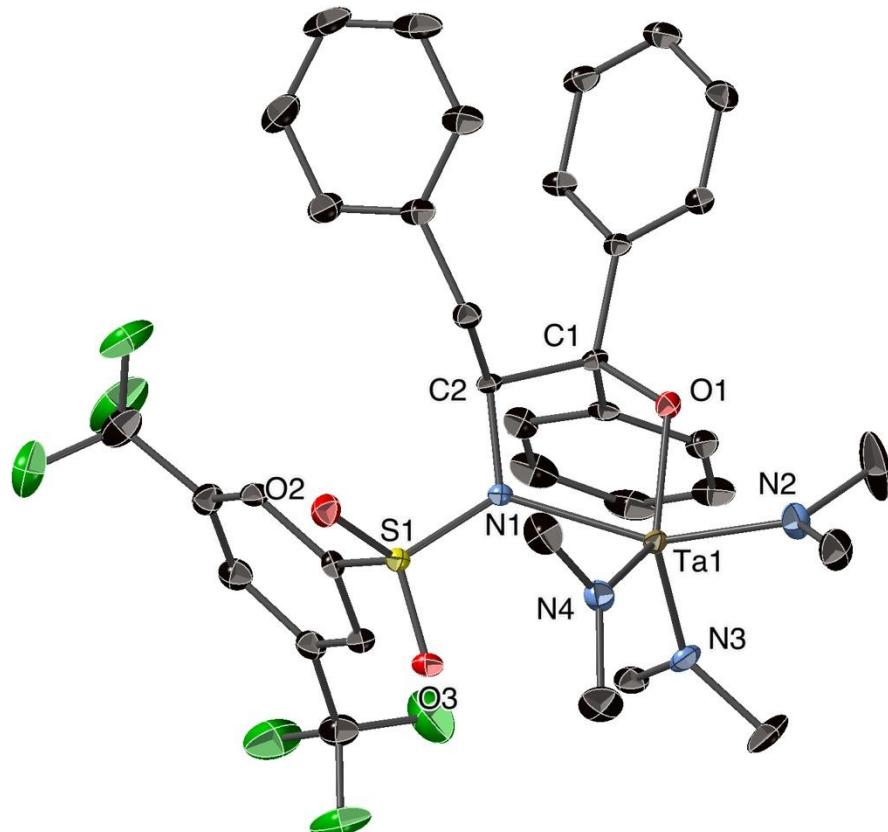
Figure 3. Thermal ellipsoid drawing of complex **TaPh3** (hydrogen atoms are omitted for clarity; ellipsoids shown at 50% probability). Selected bond distances (Å) and angles (°): Ta(1)-O(1) 1.948(3), Ta(1)-N(3) 1.958(3), Ta(1)-N(4) 1.962(3), Ta(1)-N(2) 1.993(3), Ta(1)-N(1) 2.202(3), O(1)-Ta(1)-N(3) 115.97(12), O(1)-Ta(1)-N(4) 135.16(15), N(3)-Ta(1)-N(4) 108.18(16), O(1)-Ta(1)-N(2) 87.39(13), N(3)-Ta(1)-N(2) 98.68(16), N(4)-Ta(1)-N(2) 93.60(13), O(1)-Ta(1)-N(1) 72.76(11), N(3)-Ta(1)-N(1) 102.27(13), N(4)-Ta(1)-N(1) 91.15(13), N(2)-Ta(1)-N(1) 155.86(14).

Selected metrical parameters for the four complexes are given in Table 1. Aside from

the slightly shorter bond lengths to the amide and alkoxide ligands to Ti by about 0.05 Å relative

to Ta, all four complexes exhibit a similar coordination geometry. The $Ti-NHMe_2$ bond length of

2.224(2) Å is longer than corresponding $Ta-NMe_2$ bond lengths of about 1.99 Å. $Ta-NHMe_2$

bonds have been reported at 2.410(5) Å.[50] The bond lengths between the metal centers and the

dimethylamide ligands are comparable to related complexes at 1.88-1.91 Å for Ti[48, 58-59, 68] and

1.95-1.99 Å for Ta.[45, 50, 69-70] The bond between the metal and the sulfonamide nitrogen is longer than that to the dimethylamide nitrogen by approximately 0.2 Å for all four complexes, which is consistent with previously reported sulfonamide complexes on titanium.[58-59, 68, 71] The metal oxygen bond lengths are shortened relative to similar molecules by about 0.05 Å for Ta and 0.10 Å for Ti,[45, 48, 50, 53, 58] though not outside the range of metal oxygen bonds observed.[72-73]

Table 1. Selected bond lengths and angles for **TiPh3**, **TaPh1**, **TaPh2** and **TaPh3**.

Complex	TiPh3	TaPh1	TaPh2	TaPh3
M-N(1)^a	2.115(2)	2.1952(15)	2.1720(19)	2.202(3)
M-O(1)	1.8866(18)	1.9649(15)	1.9705(17)	1.948(3)
M-N(2)^a	2.224(2)	1.9859(17)	1.993(2)	1.993(3)
M-N$_F$^{b}	1.908(2)	1.9452(18)	1.960(2)	1.958(3)
M-N$_B$^{b}	1.877(2)	1.9558(17)	1.948(2)	1.962(3)
N(1)-M-N(2)	155.24(9)	158.68(7)	156.12(8)	155.86(14)
O(1)-M-N(1)	75.91(8)	73.47(6)	73.85(7)	72.76(11)
O(1)-M-N(2)	79.82(8)	87.69(7)	84.67(8)	87.39(13)
O(1)-M-N$_F$	123.36(9)	130.78(7)	116.03(8)	135.16(15)
O(1)-M-N$_B$	120.39(10)	116.32(7)	137.55(8)	115.97(12)

^{a}N(1), the ligand nitrogen, and N(2) (NHMe$_2$ for **TiPh3** and NMe$_2$ for the tantalum complexes) are the apical atoms for an idealized trigonal bipyramidal geometry. ^{b}N$_F$ and N$_B$ are the "front" and "back" dimethylamide nitrogen atoms, N(3) or N(4), in the pseudo trigonal plane.

DOSY of complexes

The solid state structures of **TiPh3**, **TaPh1**, **TaPh2** and **TaPh3** are all monomeric, but dimerization through a bridging oxygen atom in solution is reasonable, especially for titanium, as seen previously with our bidentate amide-alkoxide ligands,[48-49] or other sulfonamide-alkoxide complexes.[53, 58] However, unlike our previously studied titanium complexes with bidentate amide-alkoxide ligands, three of the titanium complexes in this study have a coordinated dimethylamine, and all have bulky diphenyl substitution on the alkoxy carbon

which may prevent dimerization in solution. To address the solution structures of these complexes, we undertook DOSY NMR measurements.

Solutions of all eight Ti and Ta complexes were prepared in C_6D_6 and their diffusion constants were determined as an average value calculated from fits to the signal intensity for two regions of the spectra: an aryl signal and an NMe_2 signal. Additional details of the DOSY experiment are presented in the ESI. Intensity was found to decay as a function of delay time and the resulting diffusion constants are reported units of $m^2\ sec^{-1}$ using the Bruker TopSpin 3.0 software package. Hydrodynamic radii (r_h) were calculated from the diffusion constants using the Stokes-Einstein equation and are reported in Table 2.

The r_h values were not calibrated with internal standards, as can be done for more precise molecular weight determination by DOSY.[74-75] Therefore, we chose to benchmark them by determining radii for **TiPh3**, **TaPh1**, **TaPh2** and **TaPh3** by several other methods. The radius was calculated from the unit cell volume (r_{uc}), by measuring three orthogonal radii graphically within CrystalMaker (r_x), by determining the volume by summing the Van der Waals radii using the "molinfo" command within Olex2 (r_o), or by carrying out volume calculations using Gaussian (r_G). Each radius was calculated by assuming a spherical volume or averaging the three orthogonal radii. When carrying out the Gaussian calculations, electron density was integrated to 0.001 $e^-/Å^3$ using the Volume keyword using the B3LYP functional and the lanl2dz basis set. The volume and therefore the radius is defined differently by these different measures, but the average radii for the complexes are comparable (Table 2).

Table 2. Measured diffusion coefficients for **TiPh1**, **TiPh2**, **TiPh3**, **TiPh4, TaPh1, TaPh2, TaPh3**, and **TaPh4** at 25 °C in C_6D_6. Radii calculated from diffusion coefficients (r_h), from unit cell, (r_{uc}), from X-ray structure measurements (r_x), from Olex2 (r_o), and from volume Gaussian calculations (r_G).

Complex	D (m²/s)	r_h (Å)	r_{uc} (Å)	r_x (Å)	r_o (Å)	r_G (Å)
TiPh1	5.08×10^{-10}	6.8	-	-	-	-
TiPh2	5.06×10^{-10}	6.8	-	-	-	-
TiPh3	5.12×10^{-10}	6.7	6.3*	5.8	5.2	5.6
TiPh4	5.21×10^{-10}	6.6	-	-	-	-
TaPh1	5.42×10^{-10}	6.3	5.8	5.8	5.1	5.4
TaPh2	5.55×10^{-10}	6.2	5.9	5.6	5.1	5.5
TaPh3	5.25×10^{-10}	6.5	6.0	6.3	5.2	5.9
TaPh4	5.19×10^{-10}	6.6	-	-	-	-

*unit cell contains a molecule of toluene so radius is inflated relative to others.

The average hydrodynamic radius for all eight complexes is 6.6 ± 0.2 Å by our NMR techniques. Given that the r_h values for all eight complexes are similar, and the good agreement between those radii and those calculated by other methods, there is little evidence of dimerization or increased average molecularity of any of the complexes in solution. There is also no evidence of differing molecularity between the Ti and Ta complexes in solution. If the complexes were dimeric, we would anticipate an increase, though not necessarily a doubling, of the hydrodynamic radius. Other researchers have observed differences in dimer/monomer hydrodynamic radii ranging from 1.21:1 to >2:1 for a range of metal ligand combinations.[74-78] The evidence supports that the molecularity of the Ti and Ta complexes in this study are the same both in the solid state and in solution. It is reasonable that they would therefore behave similarly when coordinated to the primary amine of the substrate or the imido of the postulated intermediate during catalysis.

Intramolecular hydroamination of aminoallenes

Hydroamination was carried out using our previously described *in situ* procedures with either hepta-4,5-dienylamine (**1a**)[44, 46] or 6-methyl-hepta-4,5-dienylamine (**1b**).[44-45, 52] We have not observed differences in catalytic activity or enantioselectivity when using isolated and purified complexes relative to *in situ* catalysis. Catalyst precursor solutions were prepared by mixing stock solutions of the desired ligand and either $Ti(NMe_2)_4$ or $Ta(NMe_2)_5$ in benzene-d_6 in a J. Young NMR tube. Catalysis began by the addition of a stock solution of the aminoallene substrate in benzene-d_6 followed by heating to 110 °C (substrate **1a**) or 135 °C (substrate **1b**). All runs were carried out at 5% catalyst loading with the exception of **TiPh3** with substrate **1b**, which was also run at 10% catalyst loading due to very low conversion. The reactions were monitored by ^1H NMR spectroscopy and were quenched either when they were complete or showed no further reaction progress after 24 hours. Enantioselectivity was determined by chiral GC-MS of the corresponding benzyl derivatives. Run-to-run repeatability and repeated injections of the same sample gave errors in the calculated enantioselectivity of ±2% ee. All catalytic reactions were run in duplicate.

The catalytic hydroamination of hepta-4,5-dienylamine (**1a**) gave all three possible products (Table 3). The titanium-derived catalysts favored the tetrahydropyridine (**2a**) by a factor of 2.5:1 to 5.5:1, while the tantalum-derived catalysts gave approximately equal amounts of **2a** and the **3a** pyrrolidine products. For **TiPh4** (entry 4) and **TaPh4** (entry 8), a small impurity peak interfered with the integration of the third peak to elute, *Z*-**3a**. Including the peak in the integration would increase the %ee by about 2%. The peak was not integrated for the purposes of reporting our %ees in Table 3, but representative GC traces are shown in the ESI.

Table 3. Hydroamination of hepta-4,5-dienylamine (**1a**) at 110 ℃ with *in situ* catalysts (5 mol% catalyst) to give tetrahydropyridine **2a**, and *E*- or *Z*-α-vinylpyrrolidines *E*- or *Z*-**3a**.
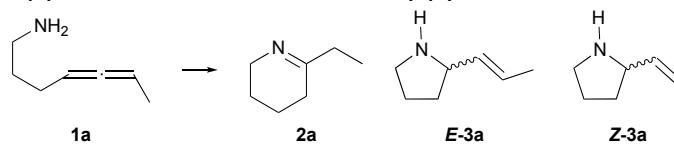
				Yield[a] (%)		
Entry	Complex	*t*/h	% conv.	**2a**	*E*-**3a**[b] (ee)	*Z*-**3a**[b] (ee)
1	**TiPh1**	64	84	60	6 (17%)	18 (5%)[c]
2	**TiPh2**	40	95	73	4 (46%)	18 (20%)[c]
3	**TiPh3**	23	98	82	5 (55%)	10 (45%)[c]
4	**TiPh4**	30	83	59	4 (19%)	20 (8%)[c]
5	**TaPh1**	30	96	49	10 (40%)	37 (17%)
6	**TaPh2**	30	97	50	10 (25%)	36 (16%)
7	**TaPh3**	23	98	48	18 (8%)	32 (21%)
8	**TaPh4**	23	95	49	10 (40%)	36 (15%)

[a]Relative amount of tetrahydropyridine:pyrrolidine determined by ^{1}H NMR, ±2%. [b]Of the benzyl derivative, determined by GC, ±2%. [b]Determined by comparison to literature values.[45, 79-81] [c]Enantiomer with longer retention time was favored. Data reported as the average of two individual runs.

The relative yield of *Z*-**3a** to *E*-**3a** ranged from 2:1 to 4.5:1, though no obvious trends are apparent for the regioselectivity. Our prior work with this substrate and bidentate amino-alcohol ligands on titanium had similar *Z*- to *E*-selectivity, although with a much lower yield of the achiral tetrahydropyridine product at 15-30%.[44] Our more recent work with tridentate imine diol ligands had a much lower *Z*- to *E*-selectivity of approximately 1:1, but again generally gave a lower yield of product **2a**.[46] The enantioselectivity of the resulting pyrrolidine products were substantially higher than previously observed by titanium-derived catalysts, up to 40-50% for *E*-**3a**.[44] However, the yields of the pyrrolidine products are too low (4-6%) to be synthetically useful. We have typically observed higher enantioselectivity of the *E*-substrates, suggesting that the regiochemistry of the substrate is at least somewhat responsible for the selectivity. Attempts to model the transition states of the reaction have been inconclusive.[82] The

enantioselectivity of the products using **TaPh1** and **TaPh4** were more than double the corresponding titanium catalysts, while for **TiPh2** and **TiPh3**, the enantioselectivity is 2-4 times higher than the corresponding tantalum catalysts for both regioisomers.

In the hydroamination of 6-methyl-hepta-4,5-dienylamine (**1b**), the titanium reactions tended to stall at about 70-90% conversion. The tantalum systems gave complete conversion with slightly higher enantioselectivity than the titanium systems. Catalysis using **TiPh3** only reached 18% conversion at 5 mol% loading (entry 3), though the enantioselectivity for pyrrolidine product was 41 %ee. Increasing the catalyst loading to 10% increased the conversion to 100%, with a lowered enantioselectivity of only 21 %ee. We observed low conversion at 5% catalyst loading in our prior report on sulfonamide ligands on titanium,[52] and in other systems,[83] but increasing the catalyst loading to 10% usually resulted in increased conversion with similar enantioselectivity rather than reducing the selectivity. With the exception of entry 3, no clear difference in enantioselectivity amongst the four ligands was observed in the titanium systems, which gave enantioselectivity of 23±4%. The 27 %ee for **TiPh4** is the highest observed enantioselectivity for an asymmetric hydroamination of an aminoallene using a titanium catalyst. The corresponding tantalum catalysts give enantiomeric excesses of 36±3%. Within error, there is no apparent influence of the sulfonamide substituents on the selectivity of the reaction, and catalysts derived from both metals favored the formation of the *S*-(-) enantiomer of product **3b**.

Table 4. Hydroamination of 6-methyl-hepta-4,5-dienylamine (**1b**) at 135 ℃ with *in situ* catalysts (5 mol% catalyst)
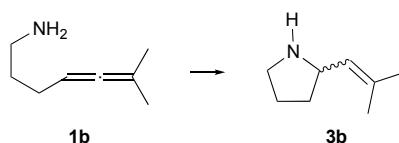
Entry	Complex	*t*/h	% conv.	% ee[a]	Config.[b]
1	**TiPh1**	18	82	18	*S*-(−)
2	**TiPh2**	32	95	24	*S*-(−)
3	**TiPh3**	106	18	41	*S*-(−)
4[c]	**TiPh3**	20	100	21	*S*-(−)
5	**TiPh4**	75	71	27	*S*-(−)
6	**TaPh1**	57	100	37	*S*-(−)
7	**TaPh2**	49	100	33	*S*-(−)
8	**TaPh3**	23	100	35	*S*-(−)
9	**TaPh4**	47	100	39	*S*-(−)

[a]Of the benzyl derivative, determined by GC, ±2%. [b]determined by comparison to literature values.[45, 79-81] [c]10 mol% catalyst loading. Data reported as the average of two individual runs.

Overall, an increase in enantioselectivity was observed in both of these new titanium and tantalum systems comparing to the previously reported analogs with either hydrogen or methyl substituents α to the oxygen.[52] These results indicate that the most important consideration for selectivity of the hydroamination reaction using these sulfonamide ligands is the substituent α to the oxygen atom and not substituents on the sulfonamide group.

One intriguing result is the substantially higher enantioselectivity of 41 %ee at 18% conversion for **TiPh3** (Table 4, entry 3). The cause of this higher selectivity at lower conversion is not currently known. Preliminary DFT calculations on both titanium and tantalum systems are consistent with [2+2] cycloaddition and cycloreversion being relatively low barrier processes with a higher barrier step to remove the product by proton transfer reactions.[82] Others have reported similar energetic profiles for early metal systems both experimentally[84] and

computationally.[85] However, the relative rates of cyclization and proton transfer are similar and temperature dependent, and other work shows that the proton transfer barrier is lower.[86-88] Schafer has recently reported that hemilabile amidate ligands are important as hydrogen bond acceptors to help mediate the protonolysis step, though in her system, the [2+2] reaction is turnover limiting.[42]

Conclusions

A series of four sterically and electronically differentiated sulfonamides were prepared. These underwent protonolysis reactions with either $Ti(NMe_2)_4$ or $Ta(NMe_2)_5$ to give their corresponding complexes. Three of the titanium complexes retain a dimethylamine ligand. The complexes were characterized by DOSY NMR and X-ray diffraction and were found to be monomeric both in solution and in the solid state, as opposed to previously characterized titanium complexes which were dimeric in the solid state. These complexes gave pyrrolidine products with higher enantioselectivity during the asymmetric hydroamination of aminoallenes compared to previously reported sulfonamide derived catalysts, but the largest contributor to the increased selectivity is the substituent α to the oxygen of the ligand, as the enantiomeric excesses are the same within error for each set of metal catalysts. While these catalysts are not yet competitive with current state of the art precious metal hydroamination catalysts, these show a promising improvement in selectivity relative to previously studied titanium catalysts.

Conflicts of Interest

There are no conflicts of interest to declare.

Experimental

General

All reagents were obtained from commercial suppliers and were purified by standard methods[89] or used as received. The ligand precursor (*S*)-2-amino-1,1,3-triphenylpropanol,[90-91] was prepared by literature procedures and recrystallized from ethanol before use. L-H$_2$**Ph1** was prepared by slight modification of literature procedures.[61] The purity of compounds was established by NMR spectroscopy and elemental analysis. Solvents were purified by vacuum transfer from sodium/benzophenone (C$_6$D$_6$) or by passage through a column of activated alumina (Innovative Technology PS-400-5-MD) and stored under nitrogen (diethyl ether, tetrahydrofuran, dichloromethane, hexane, and toluene). Column chromatography was carried out using a CombiFlash NextGen 300+ system (Teledyne ISCO). Solutions of ligands (ca. 0.05 M in C$_6$D$_6$) and substrates (ca. 1.5 M in C$_6$D$_6$) for catalysis were dried over molecular sieves overnight and stored at -35 °C. All air and/or moisture sensitive compounds were manipulated under an atmosphere of nitrogen using standard Schlenk techniques, or in a glovebox (MBraun Unilab). ^{1}H and ^{13}C NMR spectra were recorded at ambient temperature on a Brüker Avance

NEO 400 spectrometer and referenced to internal tetramethylsilane or residual solvent peaks.

Carbon assignments were made using DEPT experiments. J values are given in Hz. Polarimetry

was carried out using a JASCO P1010 instrument. IR spectroscopy was carried out using a

Thermo-Nicolet iS5 FTIR using a diamond anvil ATR accessory. GC-MS analysis was carried out

using a Hewlett Packard 5890 Series II Gas Chromatograph. Mass spectra were obtained using

an Advion expression[L] APCI Mass Spectrometer with quadrupole mass analyzer. Specific

rotation values $[\alpha]_D$, are given in 10^{-1} deg cm^2 g^{-1}. Elemental analyses were performed by

Midwest Microlab, Indianapolis, IN.

(2*S*)-2-(*p*-toluenesulfonylamino)-(1,1,3-triphenyl-1-propanol) (L-H$_2$Ph1)

IR characterization data not previously reported[61] is given here for comparison. IR (ATR,

diamond): $\nu_{SO, asym}$ = 1288 cm^{-1}, $\nu_{SO, sym}$ = 1151 cm^{-1}, ν_{SN} = 957 cm^{-1}.

(2*S*)-2-(*p*-trifluoromethylbenzenesulfonylamino)-(1,1,3-triphenyl-1-propanol) (L-H$_2$Ph2)

Under an atmosphere of N$_2$, (*S*)-2-amino-1,1,3-triphenylpropanol (8.00 mmol, 2.4280 g,

1 eq.) was dissolved in 80 mL anhydrous dichloromethane together with triethylamine (NEt$_3$)

(16.00 mmol, 2.3 mL, 2 eq.) and 4-dimethylaminopyridine (DMAP) (0.4 mmol, 0.486 g, 0.05 eq.).

After cooling to 0 °C, a solution of 4-(trifluoromethyl)benzenesulfonylchloride (8.00 mmol, 1.96

g, 1eq.) in 16 mL anhydrous dichloromethane was added slowly, and the reaction was left

stirring overnight at room temperature. The reaction was washed with 1 M HCl (20 mL),

followed by 5% NaHCO$_3$ (10 mL). The aqueous phase was extracted with 20 mL

dichloromethane twice, and the organic layer was washed with saturated NaCl solution and

dried over MgSO$_4$. Crude product was obtained by removing solvent under vacuum. The ligand

was then recrystallized from hot methanol (2.987 mmol, 1.528 g, 37%). Mp: 107-110 °C. $[\alpha]_D$=

16.4° (c= 0.0042 g / mL, EtOAc). Anal. Calcd for $C_{28}H_{24}F_3NO_3S$: C, 65.74; H, 4.73; N, 2.74. Found:

C, 65.93; H, 4.88; N, 3.01. ^{1}H NMR (400 MHz, CDCl$_3$): δ 7.52-6.97 (m, 19H, PhH), 5.11 (d, 1H, J =

8.1, NH), 4.69 (br s, 1H, CHCH$_2$Ph), 3.24 (dd, 1H, J = 3.4, 14.2, CHCH_aH$_b$Ph), 2.87 (dd, 1H, J = 6.8,

14.2, CHCH$_a$$H_b$Ph), 2.46 (brs, 1H, O$H$). ^{13}C NMR (100 MHz, CDCl$_3$): δ 144.35 (4°), 143.82 (4°),

137.09 (4°), 133.34 (4°, q, J = 33, CCF$_3$), 129.89 (CH), 128.98 (CH), 128.82 (CH), 128.33 (CH),

127.80 (CH), 127.32 (CH), 126.87 (CH), 126.08 (CH), 125.96 (q, J = 4, CH ortho to CF$_3$), 125.42

(CH), 123.48 (q, J = 271, CF$_3$), 81.06 ($\underline{C}$Ph$_2$OH), 62.26 ($\underline{C}$HCH$_2$Ph), 38.29 (CH$_2$Ph), One aromatic

CH and one aromatic 4° were not observed. ^{19}F NMR (376 MHz, CDCl$_3$): δ = 63.19. MS (APCI):

m/z 494.4 ([M-OH+H]$^+$, 60%). IR (ATR, diamond): ν$_{SO, asym}$ = 1321 cm^{-1}, ν$_{SO, sym}$ = 1155 cm^{-1}, ν$_{SN}$ =

971 cm^{-1}.

(2R)-2-(p-trifluoromethylbenzenesulfonylamino)-(1,1,3-triphenyl-1-propanol) (D-H$_2$Ph2).

The D-enantiomer was prepared according to a similar procedure starting from (R)-2-

amino-1,1,3-triphenylpropanol (1.65 mmol, 0.4980 g, 1eq.), NEt$_3$ (3.30 mmol, 0.46 mL), DMAP

(0.08 mmol, 0.0117g), and 4-(trifluoromethyl)benzenesulfonylchloride (1.65 mmol, 0.4059 g,

1eq.) in anhydrous CH$_2$Cl$_2$ (20 mL) The product was purified by chromatography (EtOAc/hexane)

(0.2277 mmol, 0.1165 g, 14%). [α]$_D$= -20.1° (c= 0.00398 g / mL, EtOAc). The ^{1}H NMR spectrum

matched that of the L-enantiomer.

(2S)-2-(3,5-bis(trifluoromethyl)benzenesulfonylamino)-(1,1,3-triphenyl-1-propanol) (L-H$_2$Ph3).

L-**H$_2$Ph3** was prepared according to a similar procedure starting from (S)-2-amino-1,1,3-

triphenylpropanol (5.284 mmol, 1.6032 g, 1 eq.), NEt$_3$ (10.568 mmol, 1.473 mL, 2 eq.), DMAP

(0.2642 mmol, 0.0323 g, 0.05 eq.), and 3,5-bis(trifluoromethyl)benzenesulfonylchloride (5.283

mmol, 1.6518 g, 1 eq.) in anhydrous CH$_2$Cl$_2$ (120 mL). The product was purified by

chromatography (EtOAc/hexane) (1.29 g, 2.23 mmol, 42%). Mp: 68.5-71 °C. $[\alpha]_D$= 29.6° (c=

0.00452 g / mL, EtOAc). Anal. Calcd for $C_{29}H_{23}F_6NO_3S$: C, 60.10; H, 4.00; N, 2.42; S, 5.53. Found:

C, 59.80; H, 4.14; N, 2.33; S, 5.76. ^1H NMR (400 MHz, CDCl$_3$): δ 7.41 (s, 3H), 7.52 – 6.91 (m, 15H,

ArH), 5.21 (br s, NH), 4.72 (dd, 1H, J = 3.3, 7.3, CHCH$_2$Ph), 3.21 (dd, 1H, J = 3.2, 14.2,

CHCH_aH$_b$Ph), 2.88 (dd, 1H, J = 7.4, 14.2, CHCH$_a$$H_b$Ph), 2.39 (br s, 1H, O$H$). ^{13}C NMR (100 MHz,

CDCl$_3$): δ 143.86 (4°), 143.58 (4°), 143.54 (4°), 136.82 (4°), 132.40 (4°, q, J = 34, CCF$_3$,), 129.78

(CH), 128.98 (CH), 128.94 (CH), 128.29 (CH), 127.95 (CH), 127.42 (CH), 126.67 (q, J = 3, $ortho$-

(F$_3$C)$_2$ArCH), 125.97 (CH), 125.58 (sept, J = 3, $para$-(F$_3$C)$_2$ArCH), 125.24 (CH), 122.59 (4°, q, J =

271, F$_3$$C$Ar), 80.99 ($CPh_2$OR), 62.97 (N$C$HCO), 38.43 ($CCH_2$). One aromatic CH was not observed.

^{19}F NMR (376 MHz, CDCl$_3$): δ 62.88. MS (APCI): m/z 304.3 ([M - (CF$_3$)$_2$C$_6$H$_3$SO$_2$ +H]$^+$, 100%). IR

(ATR, diamond): $\nu_{SO, sym}$ = 1153 cm^{-1}, ν_{SN} = 959 cm^{-1}.

(2R)-2-(3,5-bis(trifluoromethyl)benzenesulfonylamino)-(1,1,3-triphenyl-1-propanol) (D-

H$_2$Ph3).

The D-enantiomer was prepared according to a similar procedure starting from (R)-2-

amino-1,1,3-triphenylpropanol (1.65 mmol, 0.4999 g, 1 eq.), NEt$_3$ (3.30 mmol, 0.46 mL, 2 eq.),

DMAP (0.08 mmol, 0.0103 g, 0.05 eq.), and 3,5-bis(trifluoromethyl)benzenesulfonylchloride

(1.65 mmol, 0.5171 g, 1 eq.) in anhydrous CH$_2$Cl$_2$ (20 mL). The product was purified by

chromatography (EtOAc/hexane) (0.5558g, 0.959 mmol, 58%). $[\alpha]_D$= -31.1° (c= 0.0035 g / mL,

EtOAc). The ^1H NMR spectrum matched that of the L-enantiomer.

(2S)-2-(2,4,6-trimethylbenzenesulfonylamino)-(1,1,3-triphenyl-1-propanol) (L-H$_2$Ph4).

L-H$_2$Ph4 was prepared according to a similar procedure starting from (S)-2-amino-1,1-

diphenyl-3-phenylpropanol (0.9105 g, 3.001 mmol, 1 eq.) NEt$_3$ (0.835 mL, 5.991 mmol, 2 eq.)

DMAP (0.0369 g, 0.3020 mmol, 0.10 eq.), and 2,4,6-trimethylbenzenesulfonyl chloride (0.6562 g, 3.000 mmol, 1 eq.) in anhydrous CH_2Cl_2 (36 mL). The product was purified by chromatography (EtOAc/hexane) (1.0195 g, 2.099 mmol, 70%). Mp: 75.8-78.3 °C. $[\alpha]_D$ = -7.95 ° (c = 0.00352 g/mL, EtOAc). Anal. Calcd for $C_{30}H_{31}NO_3S$: C, 74.20; H, 6.43; N, 2.88. Found: C, 73.90; H, 6.40; N, 3.11. ^1H NMR (400 MHz, $CDCl_3$): δ 7.27 − 6.96 (m, 15 H, ArH), 6.72 (s, 2H, *meta*-ArH), 5.01 (d, J = 8, NH), 4.72 (dd, J = 4, 6, $CHCH_2Ph$), 3.33 (dd, J = 4, 14, $CHCH_aH_bPh$), 2.88 (dd, J = 6, 14, $CHCH_aH_bPh$), 2.60 (s, 1H, OH), 2.38 (s, 6H, $Ar(CH_3)_2$), 2.28 (s, 3H, $Ar(CH_3)$). ^{13}C NMR (100 MHz, $CDCl_3$): δ 144.14 (4°), 144.05 (4°), 141.32 (4°), 138.16 (4°), 137.18 (4°), 134.87 (4°), 131.86 (CH), 129.57 (CH), 128.66 (CH), 128.57 (CH), 128.10 (CH), 127.42 (CH), 126.81 (CH), 126.73 (CH), 125.88 (CH), 124.89 (CH), 81.16 (CPH2), 61.14 (CH), 37.90 (CH_2), 22.98 (CH_3), 20.81 (CH_3). IR (cm^{-1}): $\nu_{SO, asym}$ 1322.73 cm^{-1}, $\nu_{SO, sym}$ = 1147.70 cm^{-1}, ν_{SN} = 966 cm^{-1}.

Chiral contact shift experiments

Chiral shift studies were performed with H_2**Ph2** and H_2**Ph3** using the following procedure. L-H_2**Ph2** (20.5 mg, 0.040 mmol) was dissolved in $CDCl_3$ and examined by ^1H NMR spectroscopy. Shift reagent (S)-(+)-1-(9-anthryl)-2,2,2-trifluoroethanol (11.0 mg, 0.040 mmol, 1 eq.) was added to the solution, which was reexamined by ^1H NMR spectroscopy. An additional equivalent of shift reagent was then added to the solution for a third ^1H NMR spectrum. The same procedure was repeated with the D-H_2**Ph2** ligand. The peaks shifted without splitting throughout the process. Finally, the L- and D-H_2**Ph2** solutions with 2 eq. shift reagent were combined for a final spectrum. L-H_2**Ph2** exhibited splitting of the peaks at 2.8 and 3.2 ppm while L-H_2**Ph3** exhibited broadening of the corresponding peaks and loss of resolution but no contact shift splitting.

Complex TiPh1, Ti(NMe$_2$)$_2$(Ph1)(NHMe$_2$)

Ti(NMe$_2$)$_4$ (0.073 g, 0.323 mmol) was dissolved in ether (2 mL) and L-H$_2$**Ph1** (0.323 mmol, 0.148 g) was dissolved in ether (12 mL). Both solutions were cooled to -30 °C. The ligand was then slowly added to Ti(NMe$_2$)$_4$ solution. The solution changed color from yellow to red, and a yellow solid formed. The product was obtained as a light yellow solid by vacuum filtration (0.142 g, 0.223 mmol, 69% yield). The complex can be recrystallized from toluene. Mp: 213-215 °C. Anal. Calcd: C, 64.14; H, 6.97; N, 8.80. Found: C, 64.48, H, 7.07; N, 8.25. ^{1}H NMR (400 MHz, C$_6$D$_6$): δ 8.03 (d, 2H, J= 6.8 Hz, *ortho*-PhH), 7.19-6.92 (m, 17H, PhH), 5.13 (d, 1H, J= 7.3 Hz, CHCH$_2$Ph), 3.76 (d, 1H, J= 13.5 Hz, CHCH_aH$_b$Ph), 3.35 (s, 6H, NMe$_2$), 3.15 (dd, 1H, J= 8 Hz and 14 Hz, CHCH$_a$$H_b$Ph), 2.85 (s, 6H, NMe$_2$), 2.06 (s, 3H, PhC$H_3$) 1.92 (br d, 6H, HN(C$H_3$)$_2$). ^{13}C NMR (100 MHz, C$_6$D$_6$): δ 149.85 (4°), 147.70 (4°), 142.46 (4°), 142.02 (4°), 129.31 (CH), 129.27 (CH), 128.52 (CH), 128.48 (CH), 128.34 (CH), 127.79 (CH), 127.77 (CH), 127.57 (CH), 126.20 (CH), 126.10 (CH), 125.11 (CH), 94.52 (CPh$_2$), 71.31 (NCHCH$_2$), 46.15 (NMe$_2$), 44.49 (NMe$_2$), 41.78 (CCH$_2$), 39.97 (HN(CH$_3$)$_2$), 21.21 (PhCH$_3$). One aromatic 4° was not observed.

Complex TiPh2, Ti(NMe$_2$)$_2$(Ph2)(NHMe$_2$)

Ti(NMe$_2$)$_4$ (0.173 g, 0.770 mmol) was dissolved in diethyl ether (2 mL) and L-H$_2$**Ph2** (0.394 g, 0.770 mmol) was dissolved in diethyl ether (12 mL). Both solutions were cooled to -30 °C. Ligand was then slowly added to Ti(NMe$_2$)$_4$ solution. The solution changed color from yellow to red until yellow solid was formed, and reaction was left to stir overnight. A bright yellow solid was obtained by vacuum filtration (0.271 g, 0.393 mmol, 43%). An additional crop was obtained by reduction of solvent volume (0.216 g, 0.313 mmol, 41%). The combined solids were recrystallized from hot toluene. Mp: 166.0-169.3 °C. Anal. Calcd for C$_{32}$H$_{34}$F$_3$N$_3$O$_3$STi: C, 59.54;

H, 5.31; N, 6.51. Found: C, 59.56; H, 5.61; N, 6.97. ^{1}H NMR (400 MHz, C_6D_6): δ 7.99 (broad d, 2H,

J = 7, ArH), 7.35-6.81 (m, 17H, ArH), 5.00 (br d, J = 8, 1H, CHCH$_2$Ph), 3.72 (br d, J = 14, 1H,

CHCH_aH$_b$Ph), 3.27 (s, 6H, NMe$_2$), 3.16 (dd, J = 8, 1, 1H, CHCH$_a$$H_b$Ph), 2.76 (s, 6H, NMe$_2$) 1.85 (d, J

= 6 Hz, HN(CH_3)$_2$), 1.51 (br s, 1H, NHMe$_2$). ^{13}C NMR (100 MHz, C_6D_6): δ 149.42 (4°), 148.42 (4°),

147.33 (4°), 142.30 (4°), 132.21 (q, J = 32, 4°), 129.26 (CH), 128.63 (CH), 128.35 (CH), 128.11

(CH), 127.77 (CH), 127.67 (CH), 127.26 (CH), 126.39, (CH), 126.37 (CH), 125.77 (q, J = 4, *meta*-

CH), 125.39 (CH), 127.37* (estimated δ from peaks at 126.01 & 123.30, q, J = 271, CF$_3$), 94.54

(CPh$_2$), 71.25 (CH), 46.15 (CH$_3$), 44.46 (CH$_3$), 42.07 (CH$_2$), 40.01 (CH$_3$). ^{19}F NMR (376 MHz, C_6D_6):

δ 62.31

Complex TiPh3, Ti(NMe$_2$)$_2$(Ph3)(NHMe$_2$)·C$_7$H$_8$

Ti(NMe$_2$)$_4$ (0.200 g, 0.892 mmol) was dissolved in diethyl ether (2 mL) and L-H$_2$**Ph3**

(0.517 g, 0.892 mmol) was dissolved in diethyl ether (15 mL). Both solutions were cooled to -30

°C. The ligand was then slowly added to Ti(NMe$_2$)$_4$ solution. The solution changed color from

yellow to red. A yellow solid formed after around 6 hours, and the reaction was left to stir

overnight. A bright yellow solid was obtained by vacuum filtration (0.200 g, 0.264 mmol, 30%

yield). A second crop was obtained by reducing solvent volume (0.119 g, 0.157 mmol, 17%). The

crude ^{1}H NMR spectrum showed coordinated dimethylamine but no toluene. The combined

solids were recrystallized from hot toluene, and a toluene of solvation was observed. Mp:

146.8-150 °C. Anal. Calcd for C$_{35}$H$_{40}$F$_6$N$_4$O$_3$STi: C, 59.54; H, 5.31; N, 6.51. Calcd for

C$_{35}$H$_{40}$F$_6$N$_4$O$_3$STi·C$_7$H$_8$: C, 59.29; H, 5.69; N, 6.59. Found: C, 58.99; H, 5.78; N, 6.90. ^{1}H NMR (400

MHz, C_6D_6): δ 8.55 (broad s, 2H, *ortho*-ArH), 7.72 (s, 1H, *para*-ArH), 7.64-6.83 (m, 20H, ArH,

C$_6$$H_5$Me), 5.16 (broad d, 1H, J = 8 Hz, CHCH$_2$Ph), 3.48 (br d, 1H, J = 14, CHCH_aH$_b$Ph), 3.25 (s, 6H,

NMe$_2$), 3.09 (br dd, 1H, J = 9, 14, CHCH$_a$H$_b$Ph), 2.74 (s, 6H, NMe$_2$), 2.10 (s, 3H, C$_6$H$_5$CH$_3$), 1.80 (d,

6H, J = 6, NH(CH$_3$)$_2$), 1.44 (br s, 1H, NHMe$_2$). ^{13}C NMR (100 MHz, C$_6$D$_6$): δ 148.84 (4°), 147.90

(4°), 146.60 (4°), 141.23 (4°), 131.74 (q, J = 33, CCF$_3$); 137.52 (4° toluene), 28.95 (toluene CH),

128.41 (CH), 128.19 (toluene CH), 127.97 (CH), 127.78 (CH), 127.53 (CH), 127.24 (CH), 126.99

(unresolved q, ortho-CH), 126.77 (CH), 126.23 (CH), 126.01 (CH), 125.32 (toluene CH), 125.08

(CH), 123.64 (unresolved sept, J = 4, para-CH), 123.29* (estimated from peaks at 124.65 and

121.93, q, J = 272, CF$_3$), 94.22 (CPh$_2$), 70.63 (CH), 45.71 (CH$_3$), 43.95 (CH$_3$), 41.40 (CH$_2$), 39.54

(CH$_3$), 21.04 (toluene CH$_3$). ^{19}F NMR (376 MHz, C$_6$D$_6$): δ 62.38.

Complex TiPh4, Ti(NMe$_2$)$_2$(Ph4)

Ti(NMe$_2$)$_4$ (0.231 g, 1.03 mmol) was dissolved in toluene (2 mL) and L-H$_2$**Ph4** (0.500 g,

1.03 mmol) was dissolved in toluene (20 mL). Both solutions were cooled to -30 °C and then

combined in a Schlenk tube with additional toluene (7 mL). The reaction mixture was heated for

3 days at 65 °C. The solvent was removed in vacuo to give an orange-brown foam (0.638 g, 9.63

mmol, 95%). It has not been possible to isolate this material as a solid. ^{1}H NMR (400 MHz, C$_6$D$_6$):

δ 7.88 (d, 2H, J = 7, ArH), 7.65 (d, 2H, J = 8 Hz, ArH), 7.25-7.01 (m, 6 H, ArH), 6.75-6.65 (m, 5H,

ArH), 6.45 (s, 2H, meta-ArH), 5.47 (dd, 1H, J = 10, 4, CHCH$_2$Ph), 3.39 (s, 6H, NMe$_2$), 3.04 (s, 6H,

NMe$_2$), 2.41 (s, 6H, ortho-ArCH$_3$), 1.92 (s, 3H, para-ArCH$_3$). The benzylic protons (CH$_2$Ph) protons

are obscured by impurities. ^{13}C NMR (100 MHz, C$_6$D$_6$): δ 148.07 (4°), 147.16 (4°), 140.75 (4°),

139.21 (4°), 138.50 (4°), 137.38 (4°), 131.63 (CH), 128.77 (CH), 127.64 (CH), 127.60 (CH), 127.48

(CH), 127.23 (CH), 126.73 (CH), 126.30 (CH), 125.31 (CH), 96.84 (CPh$_2$), 71.63 (CH), 46.09 (NCH$_3$),

44.17 (NCH$_3$), 41.45 (CH$_2$), 23.16 (ArCH$_3$), 20.24 (ArCH$_3$). One aromatic CH was not observed.

Complex Ta1, Ta(NMe$_2$)$_3$(Ph1)

Ta(NMe$_2$)$_5$ (0.200 g, 0.498 mmol) was dissolved in diethyl ether (2 mL) and L-H$_2$**Ph1**

(0.228 g, 0.498 mmol) was partially dissolved in 13 mL diethyl ether. Both solutions were cooled

at -30 °C for 15 minutes. The ligand was then slowly added to Ta(NMe$_2$)$_5$ solution. The reaction

was left to stir overnight. The crude product was obtained by removing solvent (0.386 g, 0.502

mmol, 100% yield) and purified in low yield by recrystallization from ether. Mp: 197.5 - 199.0

°C. Anal. Calcd for C$_{34}$H$_{43}$N$_4$O$_3$STa: C, 53.12; H, 5.64; N, 7.29. Found: C, 53.07; H, 5.52; N, 7.09. ^{1}H

NMR (400 MHz, C$_6$D$_6$): δ 8.03 (d, 2H, J = 8, *ortho*-ArH), 7.14-6.81 (m, 17H, ArH), 5.21 (br d, 1H, J

= 8, CHCH$_2$Ph), 4.10 (br d, 1H, J = 14, CHCH_aH$_b$Ph), 3.34 (s, 18H, NMe$_2$), 3.24 (dd, 1H, J = 9, 14,

CHCH$_a$$H_b$Ph), 2.05 (s, 3H, PhC$H_3$). ^{13}C NMR (100 MHz, C$_6$D$_6$): δ 149.28 (4°), 146.42 (4°), 141.99

(4°), 141.57 (4°), 140.70 (4°), 129.36 (CH), 129.17 (CH), 129.02 (CH), 128.35 (CH), 128.09 (CH),

128.07 (CH), 127.66 (CH), 126.43 (CH), 126.35 (CH), 125.09 (CH), 93.58 (CPh2), 70.61 (CH), 45.50

(CH3), 40.21 (CH2), 21.21 (CH3). One aromatic CH carbon was not observed.

Complex Ta2, Ta(NMe$_2$)$_3$(Ph2)

Ta(NMe$_2$)$_5$ (0.250 g, 0.623 mmol) was dissolved in diethyl ether (2 mL) and L-H$_2$**Ph2**

(0.319 g, 0.623 mmol) was dissolved in diethyl ether (15 mL). Both solutions were cooled at -30

°C for 15 minutes. The ligand was then slowly added to the Ta(NMe$_2$)$_5$ solution. The reaction

was left to stir overnight. The product was obtained by removing solvent (0.520 g, 0.632 mmol,

100% yield) and purified by recrystallization from ether in low yield. Mp: 207.9-209.3 °C. Anal.

Calcd for C$_{34}$H$_{40}$F$_3$N$_4$O$_3$STa: C, 49.64; H, 4.90; N, 6.81. Found: C, 49.37; H, 4.96; N, 6.52. ^{1}H NMR

(400 MHz, C$_6$D$_6$): δ 7.93 (d, 2H, J = 8, ArH), 7.21 (d, 2H, J = 8, ArH), 7.1-6.7 (m, 15H, ArH), 5.08 (br

d, 1H, J = 8, CHCH$_2$Ph), 4.03 (br d, 1H, J = 14, CHCH_aH$_b$Ph), 3.30 (s, 18H, NMe$_2$), 3.23 (dd, 1H, J =

10, 14, CHCH$_a$H$_b$Ph). ^{13}C NMR (100 MHz, C$_6$D$_6$): δ 148.71 (4°), 146.75 (4°), 145.90 (4°), 141.66

(4°), 132.75 (q, J = 32, 4°), 129.04 (CH), 128.98 (CH), 128.29 (CH), 128.17 (CH), 128.02 (CH),

127.72 (CH), 126.61 (CH), 126.50 (CH), 125.84* (part of quartet; estimate J = 3 Hz, CH), 125.80

(CH), 125.32 (CH), 123.03* (outermost peak of CF$_3$ quartet; other peaks not observed), 93.64

(CPh$_2$), 70.80 (CH). 45.40 (CH$_3$), 40.42 (CH$_2$). ^{19}F NMR (376 MHz, C$_6$D$_6$): 62.39.

Complex Ta3, Ta(NMe$_2$)$_3$(Ph3)

Ta(NMe$_2$)$_5$ (0.200 g, 0.498 mmol) was dissolved in diethyl ether (2 mL) and L-H$_2$**Ph3**

(0.289 g, 0.498 mmol) was dissolved in diethyl ether (10 mL). Both solutions were cooled at -30

°C for 15 minutes. The ligand was then slowly added to the Ta(NMe$_2$)$_5$ solution which was then

diluted to 15 mL. The reaction was left to stir overnight. The product was obtained by removing

solvent (0.440 g, 0.494 mmol, 99% yield) and purified by recrystallization from ether. Mp 155-9

°C. Anal. Calcd for C$_{35}$H$_{39}$F$_6$N$_4$O$_3$STa: C, 47.20; H, 4.41; N, 6.29. Anal. Calcd for C$_{31}$H$_{27}$F$_6$N$_2$O$_4$STa

[Ta(NMe$_2$)(Ph3)(=O)]: C, 45.49; H, 3.32; N, 3.42. Found: C, 45.85; H, 3.89; N, 2.79. ^{1}H NMR (400

MHz, C$_6$D$_6$, 298 K): δ 8.51 (s, 2H, *ortho*-Ph*H*), 7.76 (s, 1H, *para*-Ph*H*), 7.05-6.72 (m, 15H, Ph*H*),

5.10 (br d, 1H, J = 9, C*H*CH$_2$Ph), 3.79 (br d, 1H, J = 14, CHC*H$_a$*H$_b$Ph), 3.23 (s, 18H, NMe$_2$), 3.10 (dd,

1H, J = 10, 13, CHCH$_a$*H$_b$*Ph). ^{13}C NMR (100 MHz, C$_6$D$_6$, 298 K): δ 148.41 (4°), 146.24 (4°), 145.44

(4°), 141.03 (4°), 132.34 (q, J = 33, CCF$_3$), 128.76 (br q, J = 3, ortho CH), 128.58 (CH), 128.22 (CH),

128.13 (CH), 127.68 (CH), 126.88 (CH), 126.52 (CH), 125.58 (CH), 125.41 (CH), 124.70 (sept, J =

4, para CH), 123.42 (q, J = 272 Hz, CF$_3$), 93.61 (CPh$_2$), 70.53 (CH), 45.23 (CH$_3$), 39.98 (CH$_2$). One

aromatic CH was not observed. ^{19}F NMR (376 MHz, C$_6$D$_6$): δ 62.53.

Complex Ta4, Ta(NMe₂)₃(Ph4)

Ta(NMe₂)₅ (0.200 g, 0.498 mmol) was dissolved in diethyl ether (2 mL) and ʟ-H₂**Ph4**

(0.242 g, 0.498 mmol) was dissolved in diethyl ether (5 mL). Both solutions were cooled at -30

°C for 15 minutes. The ligand was then slowly added to the Ta(NMe₂)₅ solution and the reaction

mixture was diluted to 15 mL. The reaction was left to stir overnight. The product was obtained

by removing solvent (0.436 g, 0.527 mmol, >100% yield) and purified by recrystallization from

ether. Mp: 185.4-197.4 °C. Anal. Calcd for $C_{36}H_{47}N_4O_3STa$: C, 54.27; H, 5.95; N, 7.03. Calcd for

$C_{34}H_{42}N_3O_4STa$ [Ta(NMe₂)₂(Ph4)(OH)]: C, 53.05, H, 5.50, N, 5.46. Found: C, 53.20; H, 5.79; N,

5.60. ¹H NMR (400 MHz, C_6D_6): δ 7.49 (d, 2H, J = 8, ArH), 7.38 (br s, 2H, ArH), 7.10 – 6.72 (m, 11

H, ArH), 6.73 (s, 2H, *meta*-ArH), 5.34 (dd, 1H, J = 3, 9, C*H*CH₂Ph). 3.86 (dd, 1H, J = 2, 15,

CHC*H*ₐHᵦPh), 3.42 (s, 18 H, NMe₂), 3.20 (dd, 1H, J = 9, 15, CHCHₐ*H*ᵦPh), 2.56 (s, 6H, *ortho*-CH₃),

2.04 (s, 3H, *para*-CH₃). ¹³C NMR (100 MHz, C_6D_6): δ 149.32 (4°), 146.69 (4°), 141.14 (4°), 140.82

(4°), 140.70 (4°), 137.62 (4°), 132.18 (CH), 128.85 (CH), 128.07 (CH), 127.96 (CH), 127.36 (CH),

127.28 (CH), 126.63 (CH), 126.57 (CH), 126.14 (CH), 124.92 (CH), 94.58 (CPh₂), 69.72 (CH), 45.73

(NMe₂), 40.00 (CH₂), 24.13 (CH₃), 20.82 (CH₃).

X-ray collection and refinement

A colorless block-like crystal of ʟ-H₂**Ph1** having dimensions 0.407 x 0.182 x 0.139 mm³

was grown by slow evaporation from ethanol and secured to a Mitegen micromount using

silicone vacuum grease. Its single crystal reflection data was collected at 100 K using a Rigaku

Oxford Diffraction XtaLABminiII X-ray diffractometer equipped with a HyPix-Bantam hybrid

photon counting detector and Mo K$_{\alpha1}$ radiation (λ = 0.71073 Å). Data collection strategies to

ensure completeness and desired redundancy were determined using CrysAlis[Pro].[92] Data

processing for all samples was done using CrysAlis[Pro] and multi-scan absorption corrections

were applied using the SCALE3 ABSPACK scaling algorithm.[93] The structure was solved via

intrinsic phasing methods using ShelXT[94] and refined with ShelXL[95] within the Olex2 graphical

user interface.[96] Space groups were unambiguously verified by PLATON.[97] The final structural

refinement included anisotropic temperature factors on all constituent non-hydrogen atoms.

Hydrogen atoms were attached via the riding model at calculated positions using suitable HFIX

commands.

TiPh3, **TaPh1**, **TaPh2** and **TaPh3** were crystallized from ether at -30 °C and had

dimensions of 0.300 x 0.250 x 0.150 mm^3 (**TiPh3**), 0.700 x 0.400 x 0.300 mm^3 (**TaPh1**), 0.500 x

0.250 x 0.200 mm^3 (**TaPh2**) and 0.350 x 0.250 x 0.150 mm^3 (**TaPh3**). Low-temperature

diffraction data (ϕ-and ω-scans) were collected on a Bruker AXS D8 VENTURE KAPPA

diffractometer coupled to a PHOTON II CPAD detector with Cu K_α radiation (λ = 1.54178 Å) from

an IμS micro-source (**TiPh3** and **TaPh3**) or a Bruker AXS KAPPA APEX II diffractometer coupled

to an PHOTON 100 CMOS detector with graphite monochromated Mo $K\alpha$ radiation (λ =

0.71073 Å) (**TaPh1** and **TaPh2**). The structures were solved by direct methods using SHELXS[98]

and refined against F^2 on all data by full-matrix least squares with SHELXL-2017[95] using

established refinement techniques.[99] All non-hydrogen atoms were refined anisotropically. All

hydrogen atoms were included into the model at geometrically calculated positions and refined

using a riding model. The isotropic displacement parameters of all hydrogen atoms were fixed

to 1.2 times the U value of the atoms they are linked to (1.5 times for methyl groups). Unless

otherwise noted, all disordered atoms were refined with the help of similarity restraints on the

1,2- and 1,3-distances as well as rigid bond restraints for anisotropic displacement parameters.

Thermal ellipsoid plots were generated using CrystalMaker.[100] Crystallographic data for the structures reported in this paper have been deposited with the Cambridge Crystallographic Data Centre (https://www.ccdc. cam.ac.uk) as CCDC 1970364 (L-H$_2$**Ph1**), 1970810 (**TiPh3**), 1970808 (**TaPh1**), 1970809 (**TaPh2**) and 1970811 (**TaPh3**).

DOSY NMR determination of hydrodynamic radii

DOSY experiments were performed at 298 K in a Teflon capped NMR tube (J. Young Tube) using a Bruker Avance III 400 MHz spectrometer equipped with a 5 mm BBFO SmartProbe with a z-axis gradient coil. Data were acquired and processed by using the Bruker TopSpin 3.0 software. A series of diffusion-ordered spectra were collected on samples by using the ledbpgp2s pulse sequence. Pulse-fields were incremented in 16 steps from 5 to 95 % of the maximum gradient strength in a linear ramp. The gradient length (δ) and the diffusion time (Δ) were selected to be between 1500 and 2000 μs and 100 ms, respectively. The hydrodynamic radii (r_h) were calculated from the diffusion coefficients (D) obtained from DOSY experiments according to the Stokes–Einstein equation ($D=k_BT/6\,\pi\eta r_h$). Viscosity (η) of C$_6$D$_6$ at 298 K is 0.636 Pa·s.[101]

Calculations

Theoretical studies (calculated volumes) discussed in this manuscript were carried out with the Gaussian 09[102] program suite using the WebMO[103] interface to the computing cluster at Harvey Mudd College using pdb files generated by CrystalMaker.[100] Equilibrium geometries were fully optimized by the B3LYP density functional method[104] using the lanl2dz basis set.[105-108]

Typical procedure for the hydroamination of hepta-4,5-dienylamine

Hydroamination was carried out with 5 mol% catalyst loading. Inside the glove box deuterated benzene (175 µL), Ti(NMe$_2$)$_4$ (100 µL of a 0.0375 M solution, 3.75·10^{-3} mmol), ligand (75 µL of a 0.05 M solution, 3.75·10^{-3} mmol) and hepta-4,5-dienylamine (50 µL of a 1.50 M solution, 0.075 mmol, 20 eq.) were combined in a medium-walled J. Young NMR tube. The tube was placed in a 110 ± 1 °C oil bath and monitored by ^{1}H NMR until the reaction reached completion or stalled. The E/Z ratios and percent conversion were determined by comparison with known ^{1}H NMR spectra.[109-110]

Typical procedure for the hydroamination of 6-methyl-hepta- 4,5-dienylamine

Hydroamination was carried out with 5 mol% catalyst loading. Inside the glovebox, deuterated benzene (175 µL), Ti(NMe$_2$)$_4$ (100 µL of a 0.0375 M solution, 3.75·10^{-3} mmol), ligand (75 µL of a 0.05 M solution, 3.75·10^{-3} mmol), and 6-methyl-hepta-4,5-dienylamine (50 µL of a 1.5 M solution, 0.075 mmol, 20 eq.) were combined in a medium-walled J. Young NMR tube. The tube was placed in a 135 ± 1 °C oil bath and monitored by ^{1}H NMR until the reaction reached completion or stalled. The percent conversion was determined by ^{1}H NMR spectroscopy.

Typical procedure for derivatization and determination of enantiomeric excess

The J. Young NMR tube of a completed reaction was transferred into a small vial, where benzyl bromide (9 µL, 0.08 mmol) and triethylamine (21 µL, 0.15 mmol) were added. The tube was left to sit for 18-24 hours. Isopropanol (100 µL) was added to the solution which was then filtered through glass fibers in a pipette filter. The clear solution was diluted to a total volume of 2 mL with benzene. The crude solution (1 µL) was injected on the GC capillary column

(Chiraldex B-DM, 30 m × 0.25 µm, split ratio 400, flow rate 41 cm s^{-1}, 100 °C, 8 min, 1 °C min^{-1}

to 136 °C, 10 °C min^{-1} to 180 °C, hold 20 min). The two enantiomers of E-2-propenyl-pyrrolidine

were separated with retention times of approximately 34.5 and 35.7 minutes. The two

enantiomers of Z-2-propenyl-pyrrolidine were separated with retention times of approximately

36.9 and 37.9 minutes. The two enantiomers of 2-(2-methyl-propenyl)-pyrrolidine were

separated with retention times of approximately 41.5 and 42.1 min. The absolute

stereochemistry of 2-(2-methyl-propenyl)-pyrrolidine is not known with certainty but the

preferred isomer is assigned as the S-(−)-isomer by comparison to related molecules.

References

1) Vitaku, E.; Smith, D. T.; Njardarson, J. T. *J. Med. Chem.* **2014,** *57(24)*, 10257-10274. (http://doi.org/10.1021/jm501100b)
2) Trowbridge, A.; Walton, S. M.; Gaunt, M. J. *Chem. Rev.* **2020,** *120(5)*, 2613-2692. (http://doi.org/10.1021/acs.chemrev.9b00462)
3) Hannedouche, J.; Schulz, E. *Chem. Eur. J.* **2013,** *19(16)*, 4972-4985. (http://doi.org/10.1002/chem.201203956)
4) Müller, T. E.; Hultzsch, K. C.; Yus, M.; Foubelo, F.; Tada, M. *Chem. Rev.* **2008,** *108*, 3795-3892.
5) Hultzsch, K. C. *Org. Biomol. Chem.* **2005,** *3(10)*, 1819-1824.
6) Hultzsch, K. C. *Adv. Synth. Catal.* **2005,** *347(2-3)*, 367-391.
7) Pohlki, F.; Doye, S. *Chem. Soc. Rev.* **2003,** *32(2)*, 104-14.
8) Beccalli, E. M.; Broggini, G.; Christodoulou, M. S.; Giofrè, S., Chapter One - Transition Metal-Catalyzed Intramolecular Amination and Hydroamination Reactions of Allenes. In *Advances in Organometallic Chemistry*, Pérez, P. J., Ed. Academic Press: 2018; Vol. 69, pp 1-71 (https://doi.org/10.1016/bs.adomc.2018.02.003).
9) Wolfarth, S. A.; Miner, N. E.; Wamser, N. E.; Gwinn, R. K.; Chan, B. C.; Nataro, C. *J. Organometal. Chem.* **2020,** *906*, 121049. (https://doi.org/10.1016/j.jorganchem.2019.121049)
10) Bernoud, E.; Lepori, C.; Mellah, M.; Schulz, E.; Hannedouche, J. *Catal. Sci. Technol.* **2015,** *5(4)*, 2017-2037. (http://doi.org/10.1039/c4cy01716a)
11) Hesp, K. D.; Stradiotto, M. *ChemCatChem* **2010,** *2*, 1192-1207.
12) Hong, S.; Marks, T. J. *Acc. Chem. Res.* **2004,** *37(9)*, 673-686.

13) Nguyen, H. N.; Lee, H.; Audörsch, S.; Reznichenko, A. L.; Nawara-Hultzsch, A. J.; Schmidt, B.; Hultzsch, K. C. *Organometallics* **2018**, *37(23)*, 4358-4379. (http://doi.org/10.1021/acs.organomet.8b00510)

14) Chirik, P.; Morris, R. *Acc. Chem. Res.* **2015,** *48(9)*, 2495. (http://doi.org/10.1021/acs.accounts.5b00385)

15) Hunt, A. J.; Farmer, T. J.; Clark, J. H., CHAPTER 1 Elemental Sustainability and the Importance of Scarce Element Recovery. In *Element Recovery and Sustainability*, The Royal Society of Chemistry: 2013; pp 1-28 (http://dx.doi.org/10.1039/9781849737340-00001).

16) Colonna, P.; Bezzenine, S.; Gil, R.; Hannedouche, J. *Adv. Synth. Catal.* **2020,** *362(8)*, 1550-1563. (http://doi.org/10.1002/adsc.201901157)

17) Hannedouche, J.; Schulz, E. *Organometallics* **2018,** *37(23)*, 4313-4326. (http://doi.org/10.1021/acs.organomet.8b00431)

18) Bielefeld, J.; Kurochkina, E.; Schmidtmann, M.; Doye, S. *Eur. J. Inorg. Chem.* **2019,** *2019(32)*, 3713-3718. (http://doi.org/10.1002/ejic.201900586)

19) Kaur, N.; Verma, Y.; Grewal, P.; Bhardwaj, P.; Devi, M. *Synth. Commun.* **2019,** *49(15)*, 1847-1894. (http://doi.org/10.1080/00397911.2019.1606922)

20) Edwards, P. M.; Schafer, L. L. *Chem. Commun.* **2018,** *54(89)*, 12543-12560. (http://doi.org/10.1039/C8CC06445H)

21) Perry, M. R.; Gilmour, D. J.; Schafer, L. L. *Dalton Transactions* **2019,** *48(26)*, 9782-9790. (http://doi.org/10.1039/C9DT00911F)

22) Bytschkov, I.; Doye, S. *Eur. J. Org. Chem.* **2003**, 935-946.

23) Rohjans, S. H.; Ross, J. H.; Lühning, L. H.; Sklorz, L.; Schmidtmann, M.; Doye, S. *Organometallics* **2018,** *37(23)*, 4350-4357. (http://doi.org/10.1021/acs.organomet.8b00332)

24) Reznichenko, A. L.; Hultzsch, K. C. *Organometallics* **2010,** *29(1)*, 24-27. (http://doi.org/10.1021/om9008907)

25) Odom, A. L. *Dalton Trans.* **2005,** *(2)*, 225-233.

26) Majumder, S.; Odom, A. L. *Organometallics* **2008,** *27(6)*, 1174-1177. (http://doi.org/10.1021/om700883a)

27) Swartz II, D. L.; Staples, R. J.; Odom, A. L. *Dalton Transactions* **2011,** *40(30)*, 7762-7768. (http://doi.org/10.1039/C1DT10127G)

28) Aldrich, K. E.; Odom, A. L. *Organometallics* **2018,** *37(23)*, 4341-4349. (http://doi.org/10.1021/acs.organomet.8b00313)

29) Brunner, T. S.; Hartenstein, L.; Roesky, P. W. *J. Organometal. Chem.* **2013,** *730*, 32-36. (https://doi.org/10.1016/j.jorganchem.2012.08.026)

30) Hussein, L.; Purkait, N.; Biyikal, M.; Tausch, E.; Roesky, P. W.; Blechert, S. *Chem. Commun.* **2014,** *50(29)*, 3862-3864. (http://doi.org/10.1039/C3CC48874H)

31) Manna, K.; Everett, W. C.; Schoendorff, G.; Ellern, A.; Windus, T. L.; Sadow, A. D. *J. Am. Chem. Soc.* **2013,** *135(19)*, 7235-7250.

32) Manna, K.; Eedugurala, N.; Sadow, A. D. *J. Am. Chem. Soc.* **2015,** *137(1)*, 425-435. (http://doi.org/10.1021/ja511250m)

33) Ryken, S. A.; Schafer, L. L. *Acc. Chem. Res.* **2015,** *48(9)*, 2576-2586.

34) Braun, C.; Bräse, S.; Schafer, L. L. *Eur. J. Org. Chem.* **2017,** *2017(13)*, 1760-1764.

35) Hao, H.; Thompson, K. A.; Hudson, Z. M.; Schafer, L. L. *Chem. Eur. J.* **2017,** *24(21)*, 5562-5568. (http://doi.org/10.1002/chem.201704500)

36) Lui, E. K. J.; Brandt, J. W.; Schafer, L. L. *J. Am. Chem. Soc.* **2018,** *140(15)*, 4973-4976. (http://doi.org/10.1021/jacs.7b13783)

37) Wang, X.; Chen, Z.; Sun, X.-L.; Tang, Y.; Xie, Z. *Org. Lett.* **2011,** *13(18)*, 4758-4761. (http://doi.org/10.1021/ol201731m)

38) Zhou, X.; Wei, B.; Sun, X.-L.; Tang, Y.; Xie, Z. *Chem. Commun.* **2015,** *51(26)*, 5751-5753. (http://doi.org/10.1039/C4CC10032H)

39) Michon, C.; Abadie, M.-A.; Medina, F.; Agbossou-Niedercorn, F. *J. Organometal. Chem.* **2017,** *847*, 13-27. (https://doi.org/10.1016/j.jorganchem.2017.03.032)

40) Aljuhani, M. A.; Zhang, Z.; Barman, S.; El Eter, M.; Failvene, L.; Ould-Chikh, S.; Guan, E.; Abou-Hamad, E.; Emwas, A.-H.; Pelletier, J. D. A.; Gates, B. C.; Cavallo, L.; Basset, J.-M. *ACS Catalysis* **2019,** *9(9)*, 8719-8725. (http://doi.org/10.1021/acscatal.9b02184)

41) Shen, Y.; Shepard, S. M.; Reed, C. J.; Diaconescu, P. L. *Chem. Commun.* **2019,** *55(39)*, 5587-5590. (http://doi.org/10.1039/C9CC01076A)

42) Hao, H.; Schafer, L. L. *ACS Catalysis* **2020,** *10(13)*, 7100-7111. (http://doi.org/10.1021/acscatal.0c00491)

43) LaLonde, R. L.; Sherry, B. D.; Kang, E. J.; Toste, F. D. *J. Am. Chem. Soc.* **2007,** *129(9)*, 2452-2453.

44) Hoover, J. M.; Petersen, J. R.; Pikul, J. H.; Johnson, A. R. *Organometallics* **2004,** *23(20)*, 4614-4620. (http://doi.org/10.1021/om049564s)

45) Hansen, M. C.; Heusser, C. A.; Narayan, T. C.; Fong, K. E.; Hara, N.; Kohn, A. W.; Venning, A. R.; Rheingold, A. L.; Johnson, A. R. *Organometallics* **2011,** *30(17)*, 4616-4623. (http://doi.org/10.1021/om200446v)

46) Sha, F.; Mitchell, B. S.; Ye, C. Z.; Abelson, C. S.; Reinheimer, E. W.; LeMagueres, P.; Ferrara, J. D.; Takase, M. K.; Johnson, A. R. *Dalton Trans.* **2019,** *48(26)*, 9603-9616. (http://doi.org/10.1039/C8DT05156A)

47) Hickman, A. J.; Hughs, L. D.; Jones, C. M.; Li, H.; Redford, J. E.; Sobelman, S. J.; Kouzelos, J. A.; Johnson, A. R. *Tetrahedron: Asymmetry* **2009,** *20*, 1279-1285.

48) Petersen, J. R.; Hoover, J. M.; Kassel, W. S.; Rheingold, A. L.; Johnson, A. R. *Inorg. Chim. Acta* **2005,** *358(3)*, 687-694.

49) Ho, C.; Herron, S.; Kantardjieff, K.; Johnson, A. *Inorg. Chim. Acta.* **2002,** *341*, 71-76.

50) Johnson, A. R.; Rheingold, A. L., CCDC 1575937: experimental Crystal Structure Determination, 2017, http://doi.org/10.5517/ccdc.csd.cc1pwwp4.

51) Blaser, H.-U. *Chem. Rev.* **1992,** *92*, 935-52.

52) Near, K. E.; Chapin, B. M.; McAnnally-Linz, D. C.; Johnson, A. R. *J. Organometal. Chem.* **2011,** *696(1)*, 81-86.

53) Wu, K.-H.; Gau, H.-M. *Organometallics* **2003,** *22*, 5193-5200.

54) Royo, E.; Betancort, J. M.; Davis, T. J.; Carroll, P.; Walsh, P. J. *Organometallics* **2000,** *19(23)*, 4840-4851.

55) Pritchett, S.; Gantzel, P.; Walsh, P. J. *Organometallics* **1999,** *18*, 823-831.

56) Pritchett, S.; Gantzel, P.; Walsh, P. J. *Organometallics* **1997,** *16*, 5130-5132.

57) Armistead, L. T.; White, P. S.; Gagné, M. R. *Organometallics* **1998,** *17(2)*, 216-220.

58) Armistead, L. T.; White, P. S.; Gagné, M. R. *Organometallics* **1998,** *17*, 4232-4239.

59) Hamura, S.; Oda, T.; Shimizu, Y.; Matsubara, K.; Nagashima, H. *J. Chem. Soc., Dalton Trans.* **2002,** *(7)*, 1521-1527.

60) Jaspers, D.; Saak, W.; Doye, S. *Synlett* **2012,** *23(14)*, 2098-2102. (http://doi.org/10.1055/s-0031-1290436)

61) You, J.-S.; Shao, M.-Y.; Gau, H.-M. *Tetrahedron: Asymmetry* **2001,** *12(21)*, 2971-2975. (https://doi.org/10.1016/S0957-4166(01)00522-5)

62) Tanaka, Y.; Tanaka, Y. *Chem. Pharm. Bull.* **1965,** *13(4)*, 399-405. (http://doi.org/10.1248/cpb.13.399)

63) Gowda, B. T.; Jyothi, K.; D'Souza, J. D. *Z. Naturforsch.* **2002,** *57a*, 967-978.

64) Reinheimer, E. W.; Hickman, A. J.; Moretti, J. E.; Ouyang, X.; Kantardjieff, K. A.; Johnson, A. R. *J. Chem. Crystallogr.* **2012,** *42(9)*, 911-915. (http://doi.org/10.1007/s10870-012-0334-5)

65) Reinheimer, E. W.; Kohn, A. W.; Groeneman, R. H.; Krueger, H. R.; Kantardjieff, K.; Johnson, A. R. *Mol. Cryst. Liq. Cryst.* **2016,** *629(1)*, 70-77. (http://doi.org/10.1080/15421406.2015.1106907)

66) Yao, J. W.; Copley, R. C. B.; Howard, J. A. K.; Allen, F. H.; Motherwell, W. D. S. *Acta Cryst.* **2001,** *B57*, 251-260.

67) Addison, A. W.; Rao, T. N.; Reedijk, J.; van Rijn, J.; Verschoor, G. C. *Journal of the Chemical Society, Dalton Transactions* **1984,** *(7)*, 1349-1356.

68) Schwarz, A. D.; Thompson, A. L.; Mountford, P. *Inorg. Chem.* **2009,** *48(21)*, 10442-10454. (10.1021/ic901524s)

69) Park, B. K.; Kim, H.-S.; Shin, S. J.; Min, J. K.; Lee, K. M.; Do, Y.; Kim, C. G.; Chung, T.-M. *Organometallics* **2012,** *31(23)*, 8109-8113. (10.1021/om300436p)

70) Porter, R. M.; Reid, G.; Danopoulos, A. A. *Polyhedron* **2018,** *149*, 34-38. (https://doi.org/10.1016/j.poly.2018.04.019)

71) Wu, K. H.; Gau, H. M. *Organometallics* **2004,** *23(3)*, 580-588.

72) Steinhuebel, D. P.; Lippard, S. J. *J. Am. Chem. Soc.* **1999,** *121(50)*, 11762-11772. (10.1021/ja992662y)

73) Groysman, S.; Goldberg, I.; Kol, M.; Genizi, E.; Goldschmidt, Z. *Organometallics* **2004,** *23(8)*, 1880-1890.

74) Billow, B. S.; McDaniel, T. J.; Odom, A. L. *Nature Chemistry* **2017,** *9(9)*, 837-842. (http://doi.org/10.1038/nchem.2843)

75) Hunter, S. C.; Chen, S.-J.; Steren, C. A.; Richmond, M. G.; Xue, Z.-L. *Organometallics* **2015,** *34(24)*, 5687-5696. (http://doi.org/10.1021/acs.organomet.5b00558)

76) Schlörer, N. E.; Cabrita, E. J.; Berger, S. *Angewandte Chemie International Edition* **2002,** *41(1)*, 107-109. (http://doi.org/10.1002/1521-3773(20020104)41:1<107::AID-ANIE107>3.0.CO;2-N)

77) Raya-Barón, Á.; Oña-Burgos, P.; Fernández, I., Diffusion NMR spectroscopy applied to coordination and organometallic compounds. In *Annual Reports on NMR Spectroscopy*, Webb, G. A., Ed. Academic Press: 2019; Vol. 98, pp 125-191 (http://www.sciencedirect.com/science/article/pii/S0066410319300158).

78) Miller, M.; Tshuva, E. Y. *Scientific Reports* **2018,** *8(1)*, 9705. (http://doi.org/10.1038/s41598-018-27735-0)

79) Welter, C.; Dahnz, A.; Brunner, B.; Streiff, S.; Dubon, P.; Helmchen, G. *Org Lett* **2005,** *7(7)*, 1239-42. (http://doi.org/10.1021/ol047351t)

80) Seijas, J. A.; Vazqueztato, M. P.; Castedo, L.; Estevez, R. J.; Onega, M. G.; Ruiz, M. *Tetrahedron* **1992,** *48(9)*, 1637-1642. (http://doi.org/10.1016/S0040-4020(01)88722-6)

81) Nagashima, H.; Gondo, M.; Masuda, S.; Kondo, H.; Yamaguchi, Y.; Matsubara, K. *Chem. Commun.* **2003**, 442-443.

82) Brewster, R.; Phun, G.; Cave, R. J.; Johnson, A. R., Unpublished results.

Dalton Transactions Accepted Manuscript

83) Fok, E. Y.; Show, V. L.; Johnson, A. R., Manuscript in preparation. 2020.

84) Baranger, A. M.; Walsh, P. J.; Bergman, R. G. *J. Am. Chem. Soc.* **1993,** *115(7)*, 2753-2763.

85) Tobisch, S. *Chemistry* **2007,** *13(17)*, 4884-94. (10.1002/chem.200601287)

86) Straub, B. F.; Bergman, R. G. *Angew. Chem., Int. Ed.* **2001,** *40(24)*, 4632-5.

87) Johnson, J. S.; Bergman, R. G. *J. Am. Chem. Soc.* **2001,** *123(12)*, 2923-2924.

88) Pohlki, F.; Doye, S. *Angew. Chem., Int. Ed.* **2001,** *40(12)*, 2305-2308.

89) Perrin, D. D.; Armarego, L. F., *Purification of Laboratory Chemicals*. Pergamon Press: New York, 1988.

90) Kang, Y.-F.; Liu, L.; Wang, R.; Yan, W.-J.; Zhou, Y.-F. *Tetrahedron: Asymmetry* **2004,** *15(19)*, 3155-3159. (https://doi.org/10.1016/j.tetasy.2004.08.024)

91) Liu, L.; Kang, Y.-f.; Wang, R.; Zhou, Y.-f.; Chen, C.; Ni, M.; Gong, M.-z. *Tetrahedron: Asymmetry* **2004,** *15(23)*, 3757-3761. (https://doi.org/10.1016/j.tetasy.2004.10.014)

92) *CrysAlisPro*, version 171.39.33b; Rigaku Oxford Diffraction: 2017.

93) *SCALE3 ABSPACK — A Rigaku Oxford Diffraction program for Absorption Corrections*, Rigaku Oxford Diffraction: 2017.

94) Sheldrick, G. M. *Acta Cryst.* **2015,** *A71*, 3-8. (https://doi.org/10.1107/S2053273314026370)

95) Sheldrick, G. M. *Acta Cryst.* **2015,** *C71*, 3-8. (https://doi.org/10.1107/S2053229614024218)

96) Dolomanov, O. V.; Bourhis, L. J.; Gildea, R. J.; Howard, J. A. K.; Puschmann, H. *J. Appl. Crystallogr.* **2009,** *42(2)*, 339-341. (doi:10.1107/S0021889808042726)

97) Spek, A. *Acta Cryst.* **2009,** *D65(2)*, 148-155. (http://doi.org/10.1107/S090744490804362X)

98) Sheldrick, G. *Acta. Cryst.* **1990,** *A46(6)*, 467-473. (http://doi.org/10.1107/S0108767390000277)

99) Müller, P. *Crystallography Reviews* **2009,** *15(1)*, 57-83. (http://doi.org/10.1080/08893110802547240)

100) *Crystalmaker*, 10.4.7; CrystalMaker Software Ltd, Oxford, England (www.crystalmaker.com): 2018.

101) Holz, M.; Mao, X. a.; Seiferling, D.; Sacco, A. *J. Chem. Phys.* **1996,** *104(2)*, 669-679. (http://doi.org/10.1063/1.470863)

102) Frisch, M. J.; Trucks, G. W.; Schlegel, H. B.; Scuseria, G. E.; Robb, M. A.; Cheeseman, J. R.; Scalmani, G.; Barone, V.; Petersson, G. A.; Nakatsuji, H.; Li, X.; Caricato, M.; Marenich, A. V.; Bloino, J.; Janesko, B. G.; Gomperts, R.; Mennucci, B.; Hratchian, H. P.; Ortiz, J. V.; Izmaylov, A. F.; Sonnenberg, J. L.; Williams-Young, D.; Ding, F.; Lipparini, F.; Egidi, F.; Goings, J.; Peng, B.; Petrone, A.; Henderson, T.; Ranasinghe, D.; Zakrzewski, V. G.; Gao, J.; Rega, N.; Zheng, G.; Liang, W.; Hada, M.; Ehara, M.; Toyota, K.; Fukuda, R.; Hasegawa, J.; Ishida, M.; Nakajima, T.; Honda, Y.; Kitao, O.; Nakai, H.; Vreven, T.; Throssell, K.; Montgomery, J. A.; Jr.; Peralta, J. E.; Ogliaro, F.; Bearpark, M. J.; Heyd, J. J.; Brothers, E. N.; Kudin, K. N.; Staroverov, V. N.; Keith, T. A.; Kobayashi, R.; Normand, J.; Raghavachari, K.; Rendell, A. P.; Burant, J. C.; Iyengar, S. S.; Tomasi, J.; Cossi, M.; Millam, J. M.; Klene, M.; Adamo, C.; Cammi, R.; Ochterski, J. W.; Martin, R. L.; Morokuma, K.; Farkas, O.; Foresman, J. B.; Fox, D. J., *Gaussian 16 (Revision A.03)*. Gaussian, Inc.: Wallingford, CT, 2009.

103) Schmidt, J. R.; Polik, W. F. WebMO Enterprise, version 18.0.002e, WebMO LLC: Holland, MI, USA, 2019. http://www.webmo.net/ (accessed May 4, 2020).

104) Becke, A. D. *Phys. Rev. A* **1988,** *38*, 3098-3100.

105) Dunning Jr., T. H.; Hay, P. J., In *Modern Theoretical Chemistry*, Schaefer III, H. F., Ed. Plenum: New York, 1977; pp 1-28

106) Hay, P. J.; Wadt, W. R. *J. Chem. Phys.* **1985,** *82*, 270.

107) Wadt, W. R.; Hay, P. J. *J. Chem. Phys.* **1985,** *82*, 284.

108) Hay, P. J.; Wadt, W. R. *J. Chem. Phys.* **1985,** *82*, 299.

109) Arredondo, V.; McDonald, F. E.; Marks, T. J. *J. Am. Chem. Soc.* **1998,** *120*, 4871-4872.

110) Arredondo, V.; Tian, S.; McDonald, F. E.; Marks, T. J. *J. Am. Chem. Soc.* **1999,** *121*, 3633-3639.